HØGSKOLEN I NARVIK

Expo-rational B-splines

by

Lubomir T. Dechevsky
Arne Lakså
Børre Bang

Preprint No. 1/2005
ISSN 1504-4653
Applied Mathematics

Narvik University College
NORWAY

Narvik University College
Applied Mathematics

Preprint No. 1/2005
ISSN 1504-4653

Expo-Rational B-Splines

by

Lubomir T. Dechevsky
Arne Lakså
Børre Bang

Abstract: A new type of B-spline - the expo-rational B-spline - is introduced. The heuristic motivation for its introduction comes from important similarities in several celebrated mathematical constructions originating in approximation theory, differential geometry and operator theory. The main result of the paper is the derivation of an Edgeworth and a steepest-descent/saddlepoint asymptotic expansion which shows that the expo-rational B-splines are the asymptotic limits of polynomial B-splines when the degree of the latter (or, equivalently, the number of the knots of the latter) tends to infinity. We show that, as a consequence of their nature as asymptotic limits, the new B-splines exhibit 'superproperties' by outperforming usual B-splines in a number of important aspects: for example, in constructing a minimally supported C^∞-smooth partition of unity over triangulated polygonal domains of any dimension. We illustrate this 'superperformance' by 2D and 3D graphical visualization, and discuss 'the price to pay' for it in terms of computational challenges, and how to deal with them. Finally, we present a first, non-exhaustive, list of potential applications of the new expo-rational B-spline.

Dedicated to the 60-th Anniversary of Professor Tom Lyche.

Mathematical Subject Classification (AMS 2000): Primary: 65D07; Secondary: 26A24, 26B35, 30B50, 30E20, 33F05, 41A05, 41A15, 41A20, 41A21, 41A30, 41A55, 41A58, 41A60, 41A63, 42A99, 42C40, 44A15, 46E35, 46E40, 46E50, 47A10, 47B06, 47B07, 47B10, 53A04, 53A05, 57R05, 57R10, 57R50, 58A05, 65B05, 65D05, 65D10, 65D17, 65D18, 65F50, 65L60, 65M60, 65N30, 65N50, 65T60, 65Y99, 68N19, 68Q25, 68U05, 68U07

Key words and phrases: exponential, rational, expo-rational, spline, B-spline, wavelet, multiwavelet, curve, surface, regular, regularization, non-regular, differentiable manifold, diffeomorphism, infinitely smooth, analytic, holomorphic, entire, local, global, dual, function space, Besov space, Triebel-Lizorkin space, density, distribution, real variable, complex variable, univariate, multivariate, multidimensional, interpolation, Taylor interpolation, Hermite interpolation, Padé interpolation, approximation, approximate quadratures, asymptotic approximations and expansions, Edgeworth expansion, series, special functions, Legendre transform, steepest descent, saddlepoint approximation, computer-aided geometric design, triangulation, simplectification, mesh generation, smoothing, data fitting, Cauchy integral represenation in the complex domain, Riesz-Dunford operator representation, sparse matrix, band-limited matrix, preconditioning, finite element, differential equation, ordinary, partial, boundary value problem, numerical algorithm, computational geometry, scientific computing, object-oriented, complexity

Date: June 28, 2005
• This work was supported in part by the 2003, 2004 and 2005 Annual Research Grants of the Priority R&D Group for Mathematical Modelling, Numerical Simulation and Computer Visualization at Narvik University College, Norway.
• The authors cordially thank Knut Mørken who kindly read the preliminary version of this manuscript and made important and valuable comments which have been taken in consideration in the present final preprint version.

1 Introduction

The purpose of this paper is to introduce a new type of B-splines - the *expo-rational B-splines* (*ERBS*, for short), to discuss the heuristics behind their definition, their connection to the usual polynomial B-splines, and to give a first 'aerial' overview of some of the new properties, computational specific and potential applications of these new B-splines.

In section 2 we give the definition of a particular case of ERBS, which case we choose to name the *parametric ERBS*. In section 3 we discuss several topics originating in different parts of mathematics (namely, approximation theory, differential geometry and operator theory) whose common features served to us as heuristic motivation for the introduction and study of ERBS.

The main results are concentrated in section 4 which contains the asymptotic theory connecting ERBS and polynomial B-splines. In this section is given also the definition of the general *nonparametric ERBS*.

In section 5 we discuss briefly a number of aspects in which ERBS exhibit new 'superproperties', compared to polynomial B-splines. In view of the special importance of the construction of minimally supported ERBS on triangulations, we provide also some graphical visualization of these remarkable new B-splines.

In section 6 the relevant computational issues are addressed.

Finally, section 7 contains a first discussion of potential applications of ERBS, after which the exposition is completed by a brief conclusion section.

2 Definition and Basic Properties of Univariate ERBS

Let $t_k \in \mathbb{R},\ k = 0, \dots, n+1$, and let $\overrightarrow{t} = \mathbf{t} = \{t_0, t_1, \dots, t_{n+1}\}$ be an increasing knot vector.

Definition 1. *The expo-rational B-splines (ERBS) associated with the knot vector* $\overrightarrow{t}$ *are defined by* $B_k(t) = B_k(\alpha_k, \beta_k, \gamma_k, \lambda_k, \sigma_k; t)$*, as follows:*

$$B_k(t) = \begin{cases} \int_{t_{k-1}}^{t} \varphi_{k-1}(s)ds, & t_{k-1} < t \le t_k, \\ 1 - \int_{t_k}^{t} \varphi_k(s)ds, & t_k < t < t_{k+1}, \\ 0, & \textit{elsewhere on } \mathbb{R}, \end{cases} \tag{1}$$

with

$$\varphi_k(t) = \frac{e^{-\beta_k \frac{|t-((1-\lambda_k)t_k+\lambda_k t_{k+1})|^{2\sigma_k}}{((t-t_k)(t_{k+1}-t)^{\gamma_k})^{\alpha_k}}}}{\int_{t_k}^{t_{k+1}} e^{-\beta_k \frac{|s-((1-\lambda_k)t_k+\lambda_k t_{k+1})|^{2\sigma_k}}{((s-t_k)(t_{k+1}-s)^{\gamma_k})^{\alpha_k}}} ds}, \tag{2}$$

where $\alpha_k > 0$, $\beta_k > 0$, $\gamma_k > 0$, $0 \le \lambda_k \le 1$, $\sigma_k \ge 0$, $k = 1, \dots, n$, *are the intrinsic parameters of the ERBS.*

This means that $B_k(t)$ is defined on $\mathbb{R}$ and its support is $[t_{k-1},\ t_{k+1}]$ which is the minimal possible support for continuous B-splines over $\overrightarrow{t}$ to satisfy condition P2 below.

The default values of the intrinsic parameters are $\alpha_k = \beta_k = \gamma_k = \sigma_k = 1$, $\lambda_k = \frac{1}{2}$, $k = 1, \dots, n$. The effects of modifying the values of the intrinsic parameters are addressed in subsection 5.5 and 5.6 and in [19]. An (inexhaustive) variety of different shapes of the ERBS is given in Figure 1, cases of a to f, corresponding to the sets of intrinsic parameters given in Table 1.

Intrinsic parameters					
Case/Param.	α	β	γ	λ	σ
a	1.00	1.00	1.00	0.50	1.00
b	0.50	0.10	0.30	0.30	0.80
c	0.30	4.00	3.00	0.80	0.50
d	0.40	1.70	0.60	0.90	2.00
e	1.30	0.90	0.40	0.40	0.04
f	1.40	0.20	3.50	0.99	0.50

Table 1: The sets of intrinsic parameters corresponding to the six cases in Figure 1

We mention here five basic properties of univariate ERBS:

P1. $B_k(t) \begin{cases} > 0, & t_{k-1} < t < t_{k+1}, \\ = 0, & \text{elsewhere on } \mathbb{R}, \end{cases}$
$k = 1, \dots, n;$

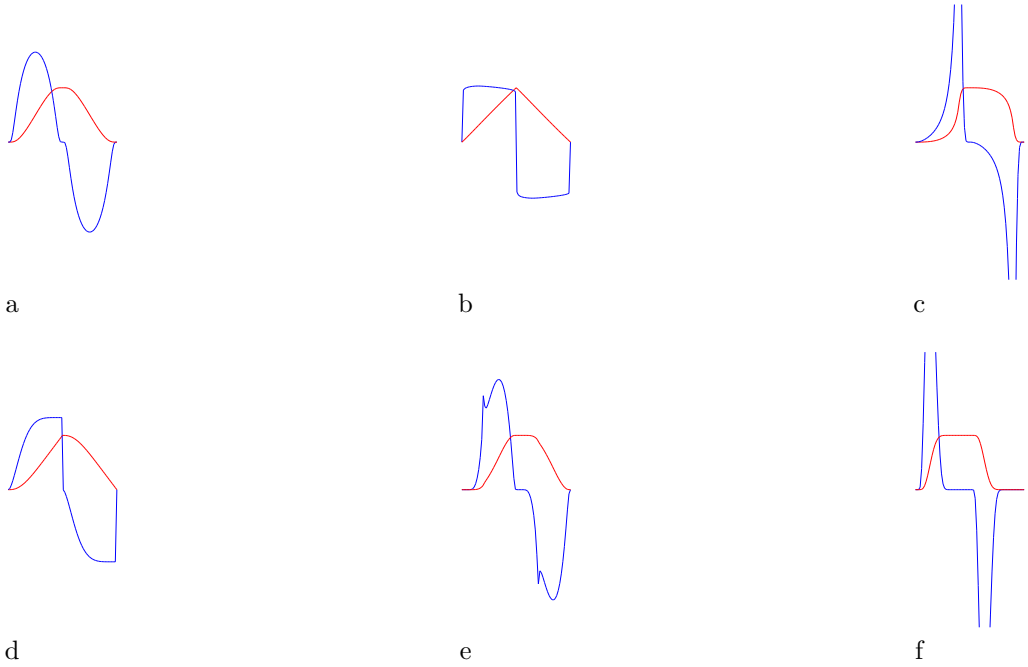

Figure 1: Some shapes of ERBS (red) and their first derivatives (blue). The respective sets of intrinsic parameters are given in Table 1. Case a corresponds to the default.

P2. $\sum_{k=1}^{n} B_k(t) = 1$, i.e.,
$B_k(t) + B_{k+1}(t) = 1,\ t_k < t \leq t_{k+1},\ k = 1, \ldots, n-1$;

P3. $B_k(t_k) = 1$ if $t_{k-1} < t_k$, and $\lim_{t \to t_k +} B_k(t) = 1$ if $t_{k-1} = t_k$, $k = 1, \ldots, n$;

P4. If $t_{k-1} < t_k < t_{k+1}$, then
$\frac{d^j}{dt^j} B_k(t_i) = 0,\ j = 1, 2, \ldots,\ k = 1, \ldots, n$;

P5. If $t_{k-1} < t_k < t_{k+1}$, then $B_k \in C_0^\infty(\mathbb{R}) \subset C^\infty(\mathbb{R})$ and B_k is analytic on $\mathbb{R} \setminus \{t_{k-1}, t_k, t_{k+1}\},\ k = 1, \ldots, n$, where C_0^∞ is the space of C^∞-smooth functions on $\mathbb{R}$ with compact support.

In the sequel of this paper it will be always assumed that the knot vector $\overrightarrow{t}$ is strictly increasing. (For the case when $\overrightarrow{t}$ is increasing, but not strictly increasing, see [19]).

Definition 2. *An ERBS (scalar-valued, vector-valued in a vector space, or point-valued in an affine frame) function $f(t)$ is defined on $(t_1, t_n]$ by*

$$f(t) = \sum_{k=1}^{n} l_k(t) B_k(t),\ t \in (t_1, t_n], \tag{3}$$

where $l_k(t)$ are local (scalar, vector-valued, or point-valued) functions defined on $(t_{k-1}, t_{k+1}),\ k = 1, \ldots, n$.

The ERBS linear combination (3) can be seen as a C^∞-smooth blending of local functions which is maximally localized, i.e., the value $f(t)$ in (3) depends on the values of only the two neighbouring local functions l_k and l_{k+1}, such that $t \in (t_k, t_{k+1})$, and only one local function l_k, if $t = t_k$. The local functions l_k are completely independent of each other, and may have similar, or very different, regularity properties. By property P5, the smoothness of $f(t),\ t \in (t_k, t_{k+1})$ will not be less than the smoothness of the less regular of the local functions l_k and l_{k+1}, while at the knots t_k, t_{k+1} the regularity of f at t_k and t_{k+1} will be as that of l_k and l_{k+1}, respectively. Moreover, in section 5 it will be shown that f in (3) interpolates every existing derivative of l_k at t_k and l_{k+1} at t_{k+1}.

In section 4 we shall see that the ERBS in Definition 1 are a particular case of a more general, non-parametric, family of bell-shaped C^∞-smooth B-splines which are defined as the asymptotic limits of usual polynomial B-splines in the case when the number of their knots tends to infinity. Taking this in consideration, we shall call the general splines *non-parametric ERBS*, while the particular type in Definition 1 will be referred to as *parametric ERBS*.

3 Heuristic Motivation for Introducing ERBS

3.1 Density of C^∞ and C_0^∞ in distribution spaces

It is a well known fact of analysis that C_0^∞ is dense in Lebesque and Sobolev spaces with metric index $p < \infty$. In general, this is not true for metric index $p = \infty$, but for all values of the metric index of these spaces, C^∞ is dense in them. One traditional way in which this is proved is to use (see, e.g., [23]) Sobolev ε-mean for $\varepsilon \to 0+$ obtained by convolving with a normalized ε-dilate of

$$\varphi(t) = \begin{cases} e^{-\frac{t^2}{1-t^2}}, & |t| < 1 \\ 0, & \text{elsewhere on } \mathbb{R} \end{cases} \tag{4}$$

which is a particular case of (2). This approach can be extended to any spaces which contain C_0^∞, resp. C^∞ as a dense subspace and are topologically embedded in D' (such as, e.g., the space S' of moderate distributions, the full range of the scales of Besov and Triebel-Lizorkin spaces, etc.). The normalization constant is given by an integral of the same type as in the denominator of the RHS of (2).

3.2 Differentiable manifolds

In the "modern" definition of differentiable manifold based on maps and atlases, which did not emerge instantly, but rather as a result of evolution (through the works of Poincare, Élie Cartan, Weyl, Whitney and others) an importent technical tool is the *C^∞-smooth partition of unity* - see, e.g., [34], Chapter 2. This construction typically uses the function φ in (4) (modulo a constant factor), and the integral

$$\psi(t) = \frac{\int_0^t \varphi(s)ds}{\int_0^\delta \varphi(s)ds},\ 0 < t < \delta,\ \delta - \text{large enough}, \tag{5}$$

see [34]. Based on the functions φ and ψ, a C^∞-smooth partition of unity is constructed with the properties P1, P2, and P5. Our Definition 1 provides such a C^∞-smooth partition of unity which has the additional property that it is *minimally supported*.

3.3 The Riesz-Dunford Integral Representation

It is fairly simple to extend the construction of a C^∞-smooth partition of unity to the case of several (including infinitely many) dimensions, by considering radial versions of φ in (4) and ψ in (5). In particular, this can be done in 2 dimensions and on the complex plane. This version of the C^∞-smooth partition of unity has been used by Friedrich Riesz to propose a general method for decomposition of the range of bounded linear operators in Banach spaces into a direct sum of closed subspaces. This idea of Friedrich Riesz was used later by Dunford to develop the operational calculus for analytic functions of such operators based on the Cauchy integral representation. In finite-dimensional spaces this calculus can be expressed by the formula in Theorem 8, section 1, Chapter VII of [12]. This formula has been inspirational for us in the design of ERBS and is closely related to the Hermite interpolatory form of functions when the local functions are (Taylor) polynomials - see section 5.

3.4 Carleman inequalities for operator resolvents

The 'classical' Carleman inequalities for resolvents in the Schatten-von Neumann ideals S_p, $0 < p \leq \infty$, of compact linear operators, are given in [13]. They assume full knowledge of the entire discrete spectrum of the compact operator. In [8] and [9] an alternative form of these inequalities, Carleman-type inequalities with minimal information about the spectrum was proposed, which assumes only the knowledge of a lower bound for the distance to the spectrum. The relevant inequalities of this type are given in Theorem 2.2.2 in [9] for the finite-dimensional case, and in the main result of [3] for the general case. In both theorems the upper bound for the resolvent norm is expressed in terms of the function $\varphi_1(t) = \exp(|\frac{c}{t}|^p)$, where $p \in (0, \infty)$ is the index of the Schatten-von Neumann class. In [9] it was shown that these results were sharp, and that the appearance of the exponential function φ_1 was deeply related with the minimality of the information about the spectrum. Any additional information about the eigenvalues and their multiplicities would result in a *polynomial, rather then exponential*, growth of $\varphi_1(t)$ with $1/t \to \infty$. This indicated that the function $\exp(|c/t|^p)$ was playing the role of one-sided (upper) asymptotic envelope of all possible polynomial upper bounds in these inequalities, and this directed us to the important work of Daniels [6] which will be discussed in the next section 4.

4 ERBS as Asymptotic Limit of Polynomial B-Splines

4.1 The 1954 paper of H. E. Daniels

The roots of contemporary spline theory can be traced back to the groundbreaking work of Schoenberg which started in the 1940s and continued through several decades. Some of his early results were published with proofs only decades later, in the 1960s and 1970s. I n particular, Schoenberg was interested in the approximation properties of polynomial cardinal spline interpolants in the case when their degree tends to infinity. In a sequence of papers in the 1970s ([29]-[32],[24]) on this topic, Schoenberg's Euler exponential splines were used as a tool in the proofs. In the last of these papers, [24], also the polynomial cardinal B-Splines were used in the case when their degree (or, equivalently, the number of knots in their support) tends to infinity. It should be noted that for the purposes of [24] B-Splines were used only as an auxiliary tool; their pointwise asymptotic limit was not studied there *per se*.

As it turns out to be the case, the pointwise asymptotic limit of polynomial uniform B-splines, with their degree tending to infinity, was already computed as early as in 1953. The respective result appears as Example 5.3 in the theoretical statistics paper [6]. It should be noted that [6] is a celebrated paper in theoretical statistics, well known to the world statistical community, and that with this paper its author H. E. Daniels has become the acknowledged founder of a whole new field in theoretical statistics, known as *small-sample asymptotics in statistics*. In view of this, it is remarkable that the relevance of this paper to spline theory has apparently remained unnoticed for half a century. In particular, the historical note in the paper [33] cited by Daniels turns out to be relevant to the early spline theory. Part of the theory in [6] has been independently re-discovered in the early 1990-es by Unser, Aldroubi and Eden in [37]. This recent study addresses one of the important aspects of the theory developed in [6] - the asymptotic convergence to a Gaussian - but it leaves out the main part of Daniels' results: the aspect of steepest-descent saddlepoint approximation and its deep connection with the Legendre transform in convex analysis. Further details about this will be given in subsection 4.2.

At the International Workshop on Wavelets in Statistics, held at Duke University on October 12-13, 1997, the first author of the present paper approached Charles A. Micchelli with a comment about potential applications of the results in [6] to deriving asymptotical expansion of the solution of refinement equations with positive coefficients. The resulting discussion between Dechevsky and Micchelli lasted for several years. In 1999, in connection with Schoenberg's papers mentioned above, Micchelli asked the question about application of Daniel's results to the asymptotic theory of B-splines when the dimension of the knot vector tends to infinity.

Due to this question, much of the credit for the discovery of the relevance of Daniels' results to the asymptotic theory of polynomial B-splines goes to Charles Micchelli.

The next two subsections contain, with some later extensions, the new results formulated in the reply letter of Dechevsky to Micchelli, dated August 7, 1999.

4.2 Edgeworth and saddlepoint approximations of B-splines

This subsection contains new, previously unpublished results, which show how the asymptotic expansion theory developed by Cramér, Khinchin and Daniels (see [6] and the references to Cramér's and Khinchin's work there), for the purposes of approximating the density of the joint distribution of N independent, identically distributed random variables, can be used to derive asymptotic expansions for polynomial B-splines with arbitrary, not necessarily strictly increasing, knot vector, in the case when its dimension (or, equivalently, the degree of the B-spline) tends to infinity.

In this first paper on this topic we shall consider only the case of a strictly increasing knot-vector (B-spline with simple knots). The general case of possible knots with multiplicity higher than 1 can be studied using the same ideas, but it is much more subtle, in view of the dependence of the regularity of the asymptotic limit on the assumptions about the multiplicities. (If the multiplicities are allowed to tend to infinity, the resulting asymptotic limit may not be C^∞-smooth in the respective knots.)

Consider the polynomial B-spline $B_{N-1}\left(\vec{\xi}_{N+1};x\right)$ of degree $N-1$, with knot-vector $\vec{\xi}_{N+1}=(\xi_0,\xi_1,...,\xi_N)$, $\dim\vec{\xi}_{N+1}=N+1$ where $\xi_0<\xi_1<...<\xi_N$, $N\in\mathbb{N}$. In the sequel, '$\sim$' denotes 'asymptotic equality'.

Theorem 1. *The polynomial B-spline has the following generalized Edgeworth asymptotic expansion*

$$NB_{N-1}\left(\vec{\xi}_{N+1};t\right)= \\ =\sqrt{\frac{N}{2\pi K''_N(\tau)}}e^{N\ K_N(\tau)-\tau t-\frac{\left(K'_N(\tau)-t\right)^2}{2K''_N(\tau)}}\ \left(1+\sum_{j=1}^{\infty}\frac{A_j}{N^{j/2}}\right), \tag{6}$$

where $\tau\in\mathbb{R}$ is a parameter, $t\in\mathbb{R}$ and:

$$A_1=\frac{1}{3!}\lambda_3(\tau)\,H_3\left[\sigma_N\left(\vec{\xi}_{N+1};\tau,t\right)\right], \tag{7}$$

$$A_2 = \frac{1}{4!}\lambda_4(\tau)\, H_4\left[\sigma_N\left(\vec{\xi}_{N+1};\tau,t\right)\right] + \frac{10}{6!}\lambda_3(\tau)^2\, H_6\left[\sigma_N\left(\vec{\xi}_{N+1};\tau,t\right)\right], \tag{8}$$

and so on, for $j = 3, 4, ...,$ *in (6); the warping* $\sigma_N\left(\vec{\xi};\tau,t\right)$ *in (6-8) is given by*

$$\sigma_N\left(\vec{\xi}_{N+1};\tau,t\right) = \left(K'_N(\tau) - t\right)\sqrt{\frac{N}{K''_N(\tau)}}, \tag{9}$$

H_l *are the classical orthogonal Hermite polynomials for* $l = 3, 4, ...,$

$$\lambda_l(\tau) = \frac{K_N^{(l)}(\tau)}{K''_N(\tau)^{l/2}},\ l = 3, 4, \ldots; \tag{10}$$

the cumulant-generating function $K_n(\tau)$ *is defined by*

$$K_N(\tau) = \frac{1}{N}\ln M_N(\tau), \tag{11}$$

where $M_N(\tau)$ *is the moment generating function, given by*

$$M_N(\tau) = e^{NK_N(\tau)} = N\int_{-\infty}^{\infty} B_{N-1}\left(\vec{\xi}_{N+1};t\right)e^{\tau t}dt. \tag{12}$$

Outline of proof: In the notations of [6], take $n = N$, $\bar{x} = t$,
$c_1 = c_2 = +\infty$ (see [6], p.632),

$$f_n(\bar{x}) = f_N(t) = NB_{N-1}\left(\vec{\xi}_{N+1};t\right), \tag{13}$$

and apply formula (4.3) in [6], p.635. □

The cumulant generating function $K_N(\tau)$ and its derivatives can be computed explicitly by a closed-form computation of the moment-generating function $M_N(\tau)$ and its derivatives. Hence, $\lambda_l(\tau)$, $l = 3, 4, ...,$ in (10) can also be computed explicitly. The next theorem provides the pattern of the explicit computation of $K_N^{(j)}(\tau)$ for the first values of j: $j = 0, 1, 2$.

Theorem 2. *For* $K_N(\tau)$*, as given in (11), there holds*

$$K'_N(\tau) = \frac{1}{N}\cdot\frac{M'_N(\tau)}{M_N(\tau)}, \tag{14}$$

$$K''_N(\tau) = \frac{1}{N}\cdot\left[\frac{M''_N(\tau)}{M_N(\tau)} - \left(\frac{M'_N(\tau)}{M_N(\tau)}\right)^2\right] = \frac{1}{N}\cdot\frac{M''_N(\tau)}{M_N(\tau)} - NK'_N(\tau)^2, \tag{15}$$

where $M_N(\tau)$*, given in (12), and its derivatives* $M'_N(\tau)$ *and* $M''_N(\tau)$ *can be computed, as follows:*

$$\begin{array}{l} M_N(\tau) = N!\varphi\left[\vec{x}_N\right] = N!\psi\left[\vec{x}_N\right] = \frac{N!}{\tau^N}\sum\limits_{k=0}^{N}\frac{e^{\tau x_k}}{w'(x_k)} = \\ N!\int_0^1\int_0^{t_1}\ldots\int_0^{t_{N-1}} e^{\left[x_0+\sum\limits_{\mu=1}^{N-1}x_\mu(t_\mu - t_{\mu+1})+x_N t_N\right]\tau}dt_N dt_{N-1}...dt_1, \end{array} \tag{16}$$

$$\vec{x}_N = \{x_0, ..., x_N\},\ x_l = N\xi_l,\ l = 0, ..., N, \tag{17}$$

$\varphi\left[\vec{x}_N\right]$ *denotes the* N*-th order divided difference of the* N*-th order Riemann-Liouville antiderivative of* $e^{\tau x}$

$$\varphi(x) = \varphi_N(\tau;x) = \frac{1}{(N-1)!}\int_{x_0}^{x}(x-\theta)^{N-1}e^{\theta\tau}d\theta, \tag{18}$$

or, equivalently, $\varphi(x)$ *is the* N*-th integral remainder in the Taylor expansion of* $\psi(x) = \psi_N(\tau;x) = \tau^{-N}e^{\tau x}$*; for* $x = Nt$*,* $w(x)$ *is defined by*

$$w(x) = w_N(x) = \prod_{k=0}^{N}(x - x_k) = N^N\omega_N(t), \tag{19}$$

$$\omega_N(\tau) = \prod_{k=0}^{N} (t - \xi_k) \tag{20}$$

$$\begin{gathered} M'_N(\tau) = \frac{N!}{\tau^N} \sum_{k=0}^{N} \frac{e^{\tau x_k}\left(x_k - \frac{N}{\tau}\right)}{w'(x_k)} = \\ N! \int_0^1 \int_0^{t_1} \dots \int_0^{t_{N-1}} e^{\left[x_0 + \sum_{\mu=1}^{N-1} x_\mu (t_\mu - t_{\mu+1}) + x_N t_N\right]\tau} \\ \times \left[x_0 + \sum_{\mu=1}^{N-1} x_\mu (t_\mu - t_{\mu+1}) + x_N t_N\right] dt_N dt_{N-1} \dots dt_1; \end{gathered} \tag{21}$$

$$\begin{gathered} M''_N(\tau) = \frac{N!}{\tau^N} \sum_{k=0}^{N} \frac{e^{\tau x_k}\left[\left(x_k - \frac{N}{\tau}\right)^2 + \frac{N}{\tau^2}\right]}{w'(x_k)} = \\ N! \int_0^1 \int_0^{t_1} \dots \int_0^{t_{N-1}} e^{\left[x_0 + \sum_{\mu=1}^{N-1} x_\mu (t_\mu - t_{\mu+1}) + x_N t_N\right]\tau} \\ \times \left[x_0 + \sum_{\mu=1}^{N-1} x_\mu (t_\mu - t_{\mu+1}) + x_N t_N\right]^2 dt_N dt_{N-1} \dots dt_1, \end{gathered} \tag{22}$$

which is strictly positive, in view of the condition $\xi_0 < \xi_N$.

Outline of proof: In formula (12), use the representation of the B-spline as divided difference and apply the 1-dimensional integral representation for the divided difference of a sufficiently smooth function. □

Using the ideas of Theorem 2, it is possible to compute the explicit dependence of $K_N^{(j)}(\tau)$, $j = 0, 1, 2, \dots$, on the knot vector $\vec{\xi}_{N+1}$, or, equivalently, on the knot vector $\vec{x}_{N+1} = N\vec{\xi}_{N+1}$, for any value of the parameter $\tau \in \mathbb{R}$. The resulting expressions are simplest for $\tau = 0$, and are given by the following result.

Theorem 3. *In the context of Theorem 1 and Theorem 2, let* $\tau = 0$. *Then, (16), (21) and (22) reduce to*

$$M_N(0) = 1, \tag{23}$$

$$M'_N(0) = x_0 + \sum_{k=1}^{N} d_k (x_k - x_{k-1}), \tag{24}$$

$$\begin{gathered} M''(0) = x_0^2 + 2x_0 \sum_{k=1}^{N} d_k (x_k - x_{k-1}) + \\ + \sum_{\mu=1}^{N} \sum_{\nu=1}^{N} d_{\mu\nu} (x_\mu - x_{\mu-1})(x_\nu - x_{\nu-1}), \end{gathered} \tag{25}$$

respectively, where

$$d_k = N! \int_0^1 \int_0^{t_1} \dots \int_0^{t_{N-1}} t_k dt_N dt_{N-1} \dots dt_1 = \frac{N + 1 - k}{N + 1}, \tag{26}$$

$$d_{\mu\nu} = N! \int_0^1 \int_0^{t_1} \dots \int_0^{t_{N-1}} t_\mu t_\nu dt_N dt_{N-1} \dots dt_1 = \frac{(N + 2 - \mu)(n + 2 - \nu)}{(n + 1)(n + 2)} \tag{27}$$

In view of the simplicity of (23), (14) and (15) also simplify, and it is easy to compute $K'_N(0)$ and $K''_N(0)$ in terms of $\vec{x}_{N+1}$ by using (24-27).

Formulae (6-12) imply that $NB_{n-1}(\vec{\xi}_{N+1}; \bullet)$ is being approximated by an appropriately dilated, translated and factored Gaussian depending on the real parameter $\tau \in \mathbb{R}$ and the real positive strictly convex C^{N-1}-smooth function $K_N(\tau)$ (which is uniquely determined by $\vec{\xi}_{N+1}$ in (11-12)), as follows.

Corollary 1. *Under the conditions of Theorem 1, the following asymptotic indentity holds*

$$NB_{N-1}(\vec{\xi}_{N+1}; t) \sim \sqrt{\frac{N}{2\pi K''_N(\tau)}} e^{N \left[K_N(\tau) - \tau t - \frac{[K'_N(\tau) - t]^2}{2K''_N(\tau)}\right]} (1 + \mathcal{O}_{\tau,t}(N^{-\frac{1}{2}})) \tag{28}$$

when $N \to +\infty$. *Moreover, the main asymptotic term in (28) can be made shape preserving, in the sense of integrating to 1 (because* $NB_{N-1}(\vec{\xi}_{N+1}; \bullet)$ *is a probability distribution density function), as follows. Denote*

$$\varphi_N(\vec{\xi}_{N+1}, \tau; t) = \sqrt{\frac{N}{2\pi K''_N(\tau)}} e^{N \left[K_N(\tau) - \tau t - \frac{[K'_N(\tau) - t]^2}{2K''_N(\tau)}\right]}, \ t \in \mathbb{R}. \tag{29}$$

Then, for any $\tau \in \mathbb{R}$,

$$\phi_N(\vec{\xi}_{N+1}, \tau; t) = \frac{\varphi_N(\vec{\xi}_{N+1}, \tau; t)}{\int_{-\infty}^{+\infty} \varphi_N(\vec{\xi}_{N+1}, \tau; \theta) d\theta}, \ t \in \mathbb{R}, \tag{30}$$

is a C^∞*-smooth approximation to* $NB_{N-1}(\vec{\xi}_{N+1}; t)$ *which retains the* $\mathcal{O}(N^{-1/2})$*-order of approximation in (28) and is shape-preserving, in the sense that it is a probalility distribution density function (i.e.,* ϕ_N *is non negative for any* $t \in \mathbb{R}$ *and integrates to* 1 *on* $\mathbb{R}$*).*

Outline of proof: The fact that the $\mathcal{O}(N^{-1/2})$-order of approximation is retained follows from the sufficiently fast convergence of $\int_{-\infty}^{\infty} \varphi_N(\vec{\xi}_{N+1}, \tau; \theta) d\theta$ to 1 as $N \to +\infty$. □

Remark 1. *The results of Theorem 1-3 and the first part of Corollary 1 correspond to the pointwise results obtained in [37]. There are, however, two important differences, as follows:*

- ***(a)*** *The present results provide an asymptotic series expansion in the powers of* $\frac{1}{\sqrt{N}}$*, while the respective pointwise results in [37] are restricted only to establishing the convergence to the main asymptotic term of this expansion. The asymptotic series expansion in (6) can be used also to obtain the* L_p*-estimates derived in [37], as well as various improvements, extensions and generalizations of these, in* L_p *and other space scales.*
- ***(b)*** *The present results are written 'in Daniels form' involving the parameter* τ*, which allows a deeper analysis of the approximation process, related, but not limited, to methods of steepest descent, saddlepoint approximation and convex analysis. The details will be given in the next subsection 4.3, and the following result is a first introduction to them.*

Corollary 2. *Under the assumption of Corollary 1, let* $\tau = \tau(t)$ *be a strictly increasing monotone* C^∞*-smooth function of* t*, such that*

$$\lim_{t \to \xi_{0+}} \tau(t) = -\infty, \qquad \lim_{t \to \xi_{N-}} \tau(t) = +\infty.$$

Then, the limits $-\infty, +\infty$ *of the integral in the denominator of the RHS of (30) can be replaced by* ξ_0 *and* ξ_N*, respectively, and* $\phi_N(\vec{\xi}_{N+1}, \tau; \bullet)$ *in (30) can be extended by* 0 *for* $t \in (-\infty, \xi_0] \cup [\xi_N, +\infty)$*, the resulting function being still* C^∞*-smooth everywhere on* $\mathbb{R}$*.*

Outline of proof: Simular to the proof of property P4 in section 2. □

Now we are finally in a position to extend Definition 1 in section 2 of the parametric ERBS to the general case of non-parametric ERBS, as follows.

Definition 3. *In the context of Definition 1, assume that the knot-vector* $\vec{t} = \vec{t}_{n+1}$ *is strictly increasing, and consider the vector* $\vec{\nu} = \vec{\nu}_n = \{N_1, \dots, N_n\}$*, the increasing knot-vectors* $\vec{\xi}_{N_k+1,k} = \{\xi_{0k}, \dots, \xi_{N_k k}\}$*,* $\xi_{0k} < \dots < \xi_{N_k k}$*,* $\xi_{0k} = t_{k-1} < t_k = \xi_{N_k k}$*, and the vector functions* $\vec{\tau} = \vec{\tau}_n = \{\tau_1(\bullet), \dots, \tau_n(\bullet)\}$ *and* $\vec{K} = \vec{K}_n = \{K_1(\bullet), \dots, K_n(\bullet)\}$*, such that, for* $k = 1, \dots, n$*,*

- ***Q1.*** $\tau_k : (t_{k-1}, t_k] \to \mathbb{R}$ *is a strictly increasing monotone* C^∞*-smooth function of its argument, with*

$$\lim_{t \to t_{k-1}^+} \tau_k = -\infty, \ \lim_{t \to t_k^-} \tau_k = +\infty;$$

- ***Q2.*** $K_k = K_{N_k k} : \mathbb{R} \to (0, \infty)$ *is computed by (11-12) for* $N = N_k$ *and* $\vec{\xi}_{N+1} = \vec{\xi}_{N_k+1,k}$ *and enjoys the following properties:* K_k *is a positive* C^∞*-smooth function of its argument and is strictly convex everywhere on* $\mathbb{R}$*. Then, the derivative of the non-parametric ERBS* $B_k(t)$ *is the asymptotic limit of* $B_{N_k k}(t) = B_{N_k k}(K_{N_k k}(\bullet), \tau_k(\bullet); t)$ *as* $N_k \to +\infty$*, where* $B_{N_k k}(t)$ *is defined by (1), with (2) generalizing to*

$$\varphi_k(t) = \varphi_{N_k k}(t) = \phi_{N_k}(\vec{\xi}_{N_k+1,k}, \tau_k; t) \tag{31}$$

as in (30), $t \in \mathbb{R}$*,* $k = 1, \dots, n$*.*

As a consequence of Definition 3, we obtain the following.

Theorem 4. *Under the assumptions of Definition 3, the non-parametric ERBS* $B_k(\bullet)$*,* $k = 1, \dots, n$*, have all the properties P1-P5.*

Outline of proof: An exercise in convergence and differentiation of integrals depending on parameters, where the compactness of $[t_{k-1},\, t_k]$ is essential. (If $t_{k-1} = -\infty$ and/or $t_k = +\infty$, additional assumptions have to be made in Definition 3 for Theorem 4 to hold.) $\square$

Remark 2. *The case $\tau = \tau_N(t)$, $\lim_{t\to\xi_{0+}} \tau_N(t) = -\infty$, $\lim_{t\to\xi_{N-}} \tau_N(t) = +\infty$, is, in some sense, an extreme case of the generalized Edgeworth expansion. The other extreme case is $\tau = 0$, which yields the classical Edgeworth approximation to $NB_{N-1}(\vec{\xi}_{N+1}; t)$ and is essentially an asymptotic-expansion enhancement of the results in [37]. As was seen in Theorem 3, this case allows particularly simple computation of $K_N(0)$ and $K''_N(0)$ in (6) and (28). However, this simple case corresponds to shape-preserving approximation by a constant bandwidth kernel which is Gaussian, i.e., not compactly supported, even if $[\xi_0, \xi_N]$ is a compact. Thus, the classical Edgeworth approximation has small absolute error, but significant relative error in the tails, and is not appropriate for generating minimally supported ERBS.*

4.3 Some important particular cases

A detailed and comprehensive analysis of the properties of the knot vector $\vec{\tau}_{N+1}$ in Definition 3 would be rather spacious and will go rather deep, taking in consideration also the fact that the Legendre transform of convex analysis gets involved in the asymptotic theory. Here we shall discuss briefly only the remarkable particular case of saddlepoint approximation, and the parametric ERBS will be shown to be a particular instance of this case when in Definition 1 $\sigma_k = 0$ is chosen.

Definition 4. *The saddlepoint approximation case corresponds to the generalized Edgeworth expansion (6) when $\tau = \tau_N(t)$ is defined implicitly as the one and only solution of the equation*

$$K'_N(\tau),\ t \in (\xi_0,\, \xi_N). \tag{32}$$

In [6] it is proved that the particular case of Definition 4 is indeed a saddlepoint approximation in the complex-variable theory of steepest-descent asymptotic approximation of Laplace integrals depending on a large parameter. Following the ideas of [6], it is possible to prove the following.

Theorem 5. *Under the conditions of Theorem 1, consider the equation $K'_N(\tau) = t$ for the unknown $\tau = \tau_N(t)$, $t \in \mathbb{R}$. Then: if $t \in \mathbb{R} \setminus (\xi_0, \xi_N)$, there are no real solutions $\tau = \tau_N(t)$; if $t \in (\xi_0,\, \xi_N)$, there exists a real solution $\tau = \tau_N(t)$ and it is unique. Moreover, if t runs through (ξ_0, ξ_N) then $\tau = \tau_N(t)$ runs through $(-\infty, \infty)$, with*

$$\lim_{t\to\xi_{0+}} \tau_N(t) = -\infty, \qquad \lim_{t\to\xi_{N-}} \tau_N(t) = +\infty \tag{33}$$

For this choice of $\tau = \tau_N(t)$ in (6), the odd coefficients A_j, $j = 2l-1$, $l = 1, 2, \ldots$, vanish, and (6) becomes

$$\begin{aligned} &NB_{N-1}(\vec{\xi}_{N+1}; t) = \\ &= \sqrt{\frac{N}{2\pi K''_N(\tau_N(t))}}\, e^{N[K_N(\tau_N(t)) - \tau_N(t)t]} \left(1 + \sum_{l=1}^{\infty} \frac{A_{2l}}{N^l}\right) = \\ &= \sqrt{\frac{N}{2\pi K''_N(\tau_N(t))}}\, e^{N[K_N(0) - \int_{K'_N(0)}^{t} \tau_N(\theta)d\theta]} \left(1 + \sum_{l=1}^{\infty} \frac{A_{2l}}{N^l}\right), \end{aligned} \tag{34}$$

and (28) becomes

$$\begin{aligned} &NB_{N-1}(\vec{\xi}_{N+1}; t) \sim \\ &\sim \sqrt{\frac{N}{2\pi K''_N(\tau_N(t))}}\, e^{N[K_N(\tau_N(t)) - \tau_N(t)t]}(1 + \mathcal{O}_t(N^{-1})) \sim \\ &\sim \sqrt{\frac{N}{2\pi K''_N(\tau_N(t))}}\, e^{N[K_N(0) - \int_{K'_N(0)}^{t} \tau_N(\theta)d\theta]}(1 + \mathcal{O}_t(N^{-1})). \end{aligned} \tag{35}$$

Outline of proof: To prove the first statement of the theorem and (33), it suffices to apply Theorems 6.1 and 6.2 in [6], pp. 638-639. The first equality in (34) follows from the definition of A_j in Theorem 1. (Note that, for this case in [6] formula (4.3) becomes (2.5).) To obtain the second equality in (34), we use the first equality and the fact that $\tau_N(t)$ is the solution of the equation $K'_N(t) = t$. Hence, since K_N is a sufficiently smooth function, $\tau_N(t)$ is also sufficiently smooth, and, by the Leibniz-Newton theorem,

$$\begin{aligned} K_N(\tau_N(t)) - \tau_N(t)t = K_N(0) - 0.K'_N(0) + \\ + \int_{K'_N(0)}^{t} [K_N(\tau_N(\theta)) - \tau_N(\theta)\theta]' d\theta = \\ = K_N(0) + \int_{K'_N(0)}^{t} [\theta\tau'_N(\theta) - \tau'_N(\theta)\theta - \tau_N(\theta)] d\theta = \\ = K_N(0) - \int_{K'_N(0)}^{t} \tau_N(\theta) d\theta, \end{aligned}$$

which proves the claim. Formula (35) follows from (34). □

We can improve the approximation of $NB_{N-1}(\vec{\xi}_{N+1};\bullet)$ in (28) to attain convergence rate higher then $\mathcal{O}(N^{-1/2})$ by including more terms in the truncation of the expansion (6). In particular, we can match the rate $\mathcal{O}(N^{-1})$ of the saddlepoint approximation in (35) by including the second term in (6). However, now the approximating function may take small negative values far enough in the tails which means that the absolute error is small but the relative error (the difference between 1 and the ratio between approximation and approximant where the approximant is strictly positive) may be large, because the approximation is not shape preserving. In contrast to this, already the first term (35) of the saddlepoint approximation (34) provides the same absolute error rate $\mathcal{O}(N^{-1})$ as well as small relative error away in the tails because of its shape-preserving properties. On the other hand, in most cases it is not possible to derive an explicit formula for $\tau = \tau_N(t),\ t \in (\xi_0, \xi_N)$, in Theorem 5. However, it is possible to obtain an explicit asymptotic formula for $\tau_N(t)$ when $t \to \xi_0+$ or $t \to \xi_N-$, as follows.

Theorem 6. *In the context of Theorem 5 (which includes the assumption that the knots ξ_k are simple), let $t \to \xi_N-$. Then, for $\omega = \omega_N$ in (20),*

$$\begin{gathered} K_N(\tau_N(t)) \sim \\ \sim \tfrac{1}{N}\ln(N!) + \tau_N(t)\xi_N - \ln\tau_N(t) - \tfrac{N-1}{N}\ln N - \tfrac{1}{N}\ln\omega'_N(\xi_N), \end{gathered} \tag{36}$$

$$K'_{N}(\tau_{N}(t)) \sim \xi_{N} - \frac{1}{\tau_{N}(t)}, \tag{37}$$

$$\tau_{N}(t) \sim \frac{1}{\xi_N - t}, \tag{38}$$

$$K''_N(\tau_N(t)) \sim \frac{1}{\tau_N(t)^2}, \tag{39}$$

$$\begin{gathered} B_{N-1}(\vec{\xi}_{N+1};t) \sim \frac{N!N}{N^N e^{-N}\sqrt{2\pi N}} \cdot \frac{(\xi_N - t)^{N-1}}{\omega'_N(\xi_N)} \sim \\ \sim \frac{N(\xi_N - t)^{N-1}}{\omega'_N(\xi_N)}. \end{gathered} \tag{40}$$

Analogous results to (36-40) can be obtained when $t \to \xi_0+$.

Outline of proof: Formulae (36-37, 39) are obtained from (14-17, 19-22) taking into account that $\tau_N(t) \to +\infty$ as $t \to \xi_N-$, and that the main asymptotic term in (16, 21-22) is the one for $k = N$, in view of the simplicity of the knots ξ_k. Next, (37) implies (38,40) where the main asymptotic term in the Stirling expansion of $N!$ in powers of $\frac{1}{N}$ has been used to obtain the second asymptotic equality in (40) □

In the particular case of uniform knots, Theorem 6 reduces to the classical asymptotic result of Daniels ([6], Example 5.3).

The results in the previous and the present subsection show that it is reasonable to use the classical Edgeworth approximation 'in the bulk' of the interior of the support of $B_{N-1}(\vec{\xi}_{N+1};\bullet)$, and the saddlepoint approximation near the boundary of this support.

The parametric ERBS provide particular instances of non-parametric ERBS. Below we study the range of the intrinsic parameters of the parametric ERBS for which its derivative is the saddle-point approximation of polynomial B-splines with appropriately distributed knot-vectors.

Theorem 7. *Let $-\infty < a < b < +\infty$, $\alpha > 0$, $\beta > 0$, $\gamma > 0$, $\sigma \geq 0$, $0 \leq \lambda \leq 1$. Then, the C^∞-smooth function*

$$\varphi(t) = \begin{cases} e^{-\beta\frac{|t-(1-\lambda)a-\lambda b|^{2\sigma}}{[(t-a)(b-t)^\gamma]^\alpha}}, & t \in (a,b) \\ 0, & t \in \mathbb{R}\setminus(a,b) \end{cases} \tag{41}$$

is the saddlepoint asymtotic limit, in the sense of (35), of a B-spline $B_{N-1}(\vec{\xi}_{N+1};\bullet)$, $a = \xi_0 < \ldots < \xi_N = b$, as $N \to +\infty$, if, and only if, the function

$$K^*(t) = \frac{|t-(1-\lambda)a-\lambda b|^{2\sigma}}{[(t-a)(b-t)^\gamma]^\alpha} \tag{42}$$

is strictly convex for every $t \in (a,b)$ and has vertical asymptotes at $t = a$ and $t = b$, with

$$\lim_{t\to a+} K^*(t) = \lim_{t\to b-} K^*(t) = +\infty \tag{43}$$

Outline of proof: Assume that K^* satisfies (42, 43) and is strictly convex on (a,b). Therefore, $K^* \in C^\infty(a,b)$. Then, by (42) the Legendre transform of K^*

$$K(\tau) = \sup_{t\in(a,b)} \{\tau t - K^*(t)\}$$

is also strictly convex and $K \in C^\infty(\mathbb{R})$ (see, e.g., [21]). Moreover, by the general theory of the Legendre transform (see [21]), $\frac{d}{d\tau}K(\tau)$ and $\frac{d}{dt}K^*(t)$ are strictly increasing, mutually inverse functions, with

$$\frac{d}{d\tau}K(\tau(t)) = t, \quad \frac{d}{dt}K^*(t(\tau)) = \tau. \tag{44}$$

By Theorem 5, there is a saddlepoint asymptotic expansion corresponding to K so that (33-35) are fulfilled. Since K and K^* are dual with respect to the Legendre transform, the same type of argument holds also in the reverse direction: from the strict convexity of $K \in C^\infty(\mathbb{R})$ with (33), it follows that $K^*(t)$ defined in (42) is strictly convex and (43) holds. □

Corollary 3. *The exact range of parameters $a, b, \alpha, \beta, \gamma, \sigma, \lambda$ in (41) for which φ in (41) satisfies the conditions of Theorem 7 is, as follows: all admissible $a, b, \alpha, \beta, \gamma$ and*

$$\sigma \begin{cases} = 0, & \lambda \in (0,1) \\ \in [0,\alpha), & \lambda = 0 \\ \in [0,\alpha\gamma), & \lambda = 1 \end{cases}$$

Outline of proof: K^* in (42) is strictly convex if, and only if,

$$\frac{d^2}{dt^2}K^*(t) = \frac{\alpha}{(t-a)^2} + \frac{\alpha\gamma}{(b-t)^2} - \frac{2\sigma}{[t-(1-\lambda)a-\lambda b]} > 0, \tag{45}$$

for all $t \in (a,b)$. In view of $\alpha > 0$, $\gamma > 0$, $\sigma \geq 0$, the case $\lambda \in (0,1)$ of the corollary follows immediately from (45). For the case $\lambda = 0$, assuming $0 \leq \sigma < \infty$, (45) is equivalent to

$$(\alpha - 2\sigma)(b-t)^2 + \alpha\gamma(t-a)^2 > 0, \text{ for all } t \in (a,b), \tag{46}$$

which includes, but is not restricted to, the case $0 \leq \sigma \leq \frac{\alpha}{2}$. However, (43) is only possible in a subcase of $0 \leq \sigma \leq \frac{\alpha}{2}$, namely $0 \leq \sigma < \frac{\alpha}{2}$, which is, therefore, the exact range for σ when $\lambda = 0$ and (43,46) are fulfilled.

A similar argument proves the case when $\lambda = 1$. □

5 Examples of new properties of ERBS

Due to their essence of being C^∞-smooth uniform asymptotic limits (together with their derivatives of every order) of polynomial B-splines, ERBS behave as 'super splines', geometrically outperforming every polynomial spline (cf. also the discussion in subsection 3.4). An important part of the benefits of this 'super spline' performance is that:

(a) many theoretical constructions (e.g., Hermite and Padé interpolants, or smooth bivariate B-splines on triangulations) become simpler, and more transparent - even explicitly computable in closed form - in the case of ERBS;

(b) algorithm design, programming and geometric modelling with ERBS is *much simpler* than with polynomial B-spline.

In support of claim (a), formulated above, in this section we give several examples of 'theoretical superproperties' of ERBS. Some first arguments in favour of claim (b) are discussed in [19]. A detailed and comprehensive systematic study of properties of ERBS will be conducted elsewhere.

5.1 Diversity of local function spaces

If for a fixed $k = 1, \ldots, n$ we limit the consideration in Definition 2 only to C^∞-smooth local curves l_k in (3), the *maximal local function space* $\mathcal{F}(B_k)$ in (3) is the linear space of all $f_k \in C^\infty(t_{k-1}, t_{k+1})$ such that the right-hand limit at t_{k-1} and the left-hand limit at t_{k+1} exist for $[f_k(t)B_k(t)]^{(j)}$, and

$$\lim_{t \to t_{k-1}+} \frac{d^j}{dt^j}[f_k(t)B_k(t)] = \lim_{t \to t_{k+1}-} \frac{d^j}{dt^j}[f_k(t)B_k(t)] = 0, \tag{47}$$

for all $j = 0, 1, \ldots$. This is a very large, infinite-dimensional, separable function space satisfying

$$C^\infty[t_{k-1}, t_{k+1}] \subset \mathcal{F}(B_k) \subset C^\infty(t_{k-1}, t_{k+1}), \tag{48}$$

and it contains all algebraic and trigonometric polynomials (restricted to $[t_{k-1}, t_{k+1}]$), all rational functions without poles in (t_{k-1}, t_{k+1}) (including NURBS and rational functions with poles at t_{k-1} and/or t_{k+1}) and a rich variety of special functions, including Schoenberg's Euler exponential splines, as well as all solutions of boundary value problems on $[t_{k-1}, t_{k+1}]$ for constant-coefficient ODEs of arbitrary finite order (thus, including also all solutions of constant-coefficient Sturm-Liouville problems of every order on $[t_{k-1}, t_{k+1}]$). It is possible to consider local curves which are linear combinations of ERBS defined over a (strictly) increasing knot vector $\vec{\tau}_k = \{\tau_{k,0}, \ldots, \tau_{k,n_k+1}\}$, such that $\tau_{k,0} < \tau_{k,1} = t_k < \ldots < t_{k+1} = \tau_{k,n_k} < \tau_{k,n_k+1}$, $k = 1, \ldots, n$, which gives rise to a 2-level ERBS. Iterating this procedure yields multilevel ERBS.

From the point of view of geometric modelling, it is useful to compare the control polygon of a Bezier or B-spline curve with the control polygon of an ERBS curve. In the former case, the control polygon is, as well known, a piecewise linear polygon in $\mathbb{R}^3$ which is *constant*, i.e., *does not depend on the parameter t of the curve*, and the curve lies in the convex hull of this polygon. In the latter case (ERBS curve) the control polygon is *variable, i.e., depends on the parameter t of the curve* - see Figure 2. For every fixed value of t this polygon is the convex hull of two points, i.e., a segment, and the point $P(t)$ on the curve is in this convex hull, i.e., in the segment - see Figure 2. Thus, the control polygon of the ERBS curve for all t is a band of a ruled surface with parametrization $\vec{r}(u, v)$ where $u = t$, $v \in [0, 1]$ is the linear parameter of the ruled surface, and the ERBS curve is a parametric curve on this surface, with parametrization $\vec{r}(u(t), v(t)) = \vec{r}(t, v(t))$ - see Figure 2.

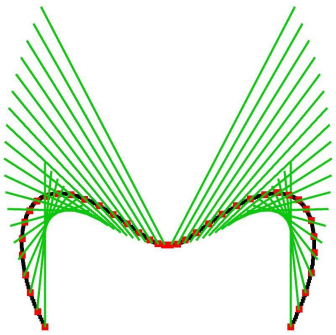

Figure 2: An ERBS parametric curve and its variable control polygon

5.2 Interpolation and approximation

ERBS and their derivatives of every order are non-regular non-analytic C^∞-smooth curves at the knots t_k, $k = 0, \ldots, n+1$, and are regular analytic curves between the knots. This fact, remarkable in itself, is very important and beneficial, both theoretically and practically, as demostrated by the observations in the remaining part of this subsection.

The ERBS curve $f(t)$ in (3) is the Hermite interpolant of every order of its local curves $l_k(t)$ in the knots t_k, $k = 1, \ldots, n$, i.e.,

$$\frac{d^j}{dt^j} f(t_k) = \frac{d^j}{dt^j} l_k(t_k), \; k = 1, \ldots, n, \; j = 0, 1, \ldots. \tag{49}$$

In particular, if $l_k \in P_{r_k}(t_{k-1}, t_{k+1})$ - the space of algebraic polynomials of degree $r_k - 1$, $r_k = 1, 2, \ldots$, $k = 1, \ldots, n$, then the Hermite interpolant (3) of a sufficiently smooth function g at the knot t_k with multiplicity r_k, $k = 1, \ldots, n$, can be written explicitly as

$$f(t) = \sum_{k=1}^{n} \left[\sum_{j=0}^{r_k - 1} \frac{(t - t_k)^j}{j!} g^{(j)}(t_k) \right] B_k(t), \qquad t \in [t_1, t_n], \tag{50}$$

or, in other words, global Hermite interpolation is achieved by C^∞-smooth blending with $B_k(t)$ of local Taylor interpolants (cf. also the discussion in subsection 3.3) which is the same for every choice of $r_k = 1, 2, \ldots,\ k = 1, \ldots, n$. The canonical dual functionals and polar form (blossom) (see, e.g., [20]) can be written directly from the RHS (right-hand side) of (50). In the extreme case when $r_k = +\infty,\ k = 1, \ldots, n$, Hermite interpolation by ERBS is exact on the infinite-dimensional space $\mathcal{A}(\vec{t}_{n+1})$ of all functions defined on $[t_1, t_n]$, C^∞-smooth at the knots and analytic elsewhere on $[t_1, t_n]$. Moreover, for every $f \in \mathcal{A}(\vec{t}_{n+1})$, the following identity holds:

$$f(t) = \sum_{k=1}^{n} \left[\sum_{j=0}^{\infty} \frac{(t-t_k)^j}{j!} f^{(j)}(t_k) \right] B_k(t), \qquad t \in [t_1, t_n], \tag{51}$$

In the other extreme case, $r_k = 1,\ k = 1, \ldots, n$ (Lagrange interpolation), there is another remarkable phenomenon: the curve

$$\vec{f}(t) = \sum_{k=1}^{n} \vec{c}_k B_k(t), \qquad t \in \mathbb{R}, \tag{52}$$

where $\vec{c}_k$ are constants (2D or 3D vectors or points, etc.), is piecewise linear, and geometrically coincides with the piecewise linear polynomial B-spline curve, yet (52) posseses a C^∞-smooth parametrization! The reason why this is possible is, of course, that this parametrization is not regular in the knots. More details about this remarkable 'super G-continuity' at the knots of ERBS curves and surfaces are given in [19]; its potential applications are discussed in Section 7 below. In the RHS of Figure 3 is given the graph of an ERBS-based Lagrange interpolant. It has a piecewise linear graph (geometric place of points) and a C^∞-smooth parametrization. At the LHS of Figure 3 is the graph of the first derivative of the parametrization, which is a 3D star centered at the origin of $\mathbb{R}^3$. The graphs of the parametrization derivatives of all orders are also origin-centered stars with the same number and direction, but possibly different length, of the beams.

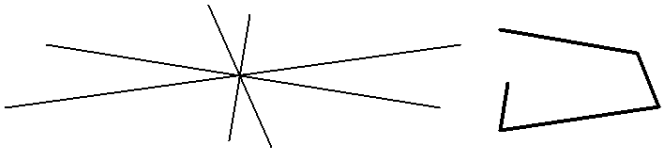

Figure 3: ERBS-based Lagrange interpolant in 3D (right): the graph is piecewise linear, but the parametrization on it is C^∞-smooth. On the left: the 3D star, centered at the origin, is the graph of the first derivative of the C^∞-smooth parametrization.

Expo-rational curves and surfaces 'bend' much faster then polynomial-based ones. Due to this, Hermite interpolation by ERBS provides a much better tool for local approxiation than its analogue with polynomials and polynomial B-splines. This feature is additionally considerably enhanced when the local curves (or surface patches) are based on rational functions. The respective Padé interpolants are indeed a 'super-tool' for combined interpolation and local approximation. They interpolate the data sets (even those forcing an overfit) in a minimalistic yet smooth way, without the additional local alternating oscillation typical for locally polynomial curves and surfaces, and without Gibbs phenomena at one-sided discontinuity points, while retaining C^∞-smoothness everywhere. Rational functions are known to be a much better tool for approximation of non-smooth functions (see [22], [38], [35], [36]) then polynomials. At the same time, they approximate $e^x,\ x \in (-\infty, 0]$, with an even higher exponential convergence rate (see [27]). These two facts, taken together with the definition of $\varphi_k(t)$ in (2), show that ERBS with rational l_k's in (3) are at least as good as rational functions at local approximation of both non-smooth and smooth functions. In the case of Hausdorff approximation in the vector-valued case (parametric curves in 2D or 3D), the ERBS Lagrange interpolation (52) is exact on piecewise linear functions with knots at $t_k,\ k = 1, \ldots, n$, which provides *an example in which ERBS essentially outperform rational functions*. The multiplicity r_k of a knot t_k has a different meaning for ERBS in (50), compared to its meaning in the case of polynomial B-splines. The same is true for knot insertion and removal. In the case of ERBS, property P4 ensures that the patch on (t_k, t_{k+1}) is 'detached' from its neighbours, in the sense that each subinterval (t_k, t_{k+1}) has its own set of intrinsic parameters, and these sets are independent of each other. Thus, introducing a new knot $\xi \in (t_l, t_{l+1})$ with multiplicity ρ_ξ for the ERBS curve in (50) is achieved by defining a new ERBS centered at ξ and supported at $[t_{l-1}, t_l]$ and modifying 'the right half' of B_{l-1} and 'the left half' of B_l, so that P1 is again fulfilled on $[t_l, t_{l+1}]$. This is possible, because of the above-mentioned 'detachment' property. The pieces are then fixed together by Hermite interpolation at the knots t_l, ξ and t_{l+1} with multiplicities r_l, ρ_ξ and r_{l+1}, respectively. The case when $\xi = t_l$ means simply that at t_l the multiplicity r_l in (50) is increased to $r_k + \rho_\xi$. Knot removal is obtained by the same procedure, taken in the reverse direction.

The effect of this type of knot insertion/removal with ERBS is the same as with polynomial B-splines: a tradeoff between interpolation and fitting of the data. It should not be mixed up with the case of non-strictly increasing knot vector $\vec{t}$ in Definition 1 which is discussed in [19] and which, in terms of the asymptotic theory in Section 4 would correspond to the case of a non-simple knot ξ_l of the polynomial B-spline, with multiplicity tending to infinity as $N \to +\infty$.

5.3 Shape preservation

'Shape preservation' is understood here as preservation of non-negativity, monotonicity, convexity, global maximal and minimal values, and values of the integral. Variation diminution is also of interest. All this can be achieved by the use of a Bezier form of ERBS. This form is simplest to describe for the case (50) of polynomial l_k's in (3), although it can be defined also for other local curves, especially, rational curves. The Hermite interpolatory form (50) of $f(t)$ can be transformed into Bezier form of $f(t)$, as follows,

$$f(t) = \sum_{k=1}^{n} \left[\sum_{i=0}^{r_k-1} c_{ki} b_{r_k,i}(t) \right] B_k(t), \qquad t \in [t_1, t_n], \tag{53}$$

where $b_{r_k,i},\ i = 0, \ldots, r_k - 1$, are the Bernstein polynomials of degree $r_k - 1$ on $[t_{k-1}, t_{k+1}],\ k = 1, \ldots, n$. The coefficients of the Bezier form can be obtained from the coefficients of the Hermite form, and vice versa, via the n changes of basis between the Taylor monomial basis $\frac{(t-t_k)^i}{i!},\ i = 0, \ldots, r_k - 1$, and the respective Bernstein basis $b_{r_k-1,j}(t),\ j = 0, \ldots, r_k - 1$,
$k = 1, \ldots, n$. Due to the independence of the l_k's in (3), these n basis transformations are independent of each other, and can be done in parallel. Since the local curves in (53) are Bezier curves, in the case of ERBS the de Boor-Cox algorithm reduces to n applications of the de Casteljau algorithm, one for each closed interval $[t_{k-1}, t_{k+1}]$, going to depth $r_k,\ k = 1, \ldots, n$. These n de Casteljau iterative processes are again independent of each other, and can be done in parallel. The transformations between the two forms (50) and (53) are fast, and provide the designer with the additional option to be able to edit curves and surfaces by interactively modifying both the Bezier control polygon and the Hermite interpolatory polygon in real time.

ERBS preserve the nice variation-diminution property of polynomial B-splines. In particular, the operator given by the RHS of (53) with

$$c_{ki} = \begin{cases} f\left(t_{k-1} + i\dfrac{t_{k+1} - t_{k-1}}{r_k - 1}\right), & i = 0, \ldots, r_k - 1, \quad r_k = 2, 3, \ldots, \\ f(t_k), & r_k = 1, \end{cases} \tag{54}$$

$k = 1, \ldots, n$, provides a simple example of an ERBS variation-diminishing approximation operator.

ERBS curves and surfaces can approach the extreme points of the convex hull of their control points much more closely then polynomial B-spline curves and surfaces. Because of this, the convergence of the control polygon/polyhedron to the ERBS curve/surface is much faster then with polynomial B-splines. (The extreme case is again Lagrange interpolation, i.e., $r_k = 1,\ k = 1, \ldots, n$, in (53).) In view of the explicit asymptotic theory of the non-parametric ERBS in Section 4, the study of the stability constants and condition numbers for ERBS bases may shed additional light on some unsolved problems about the sharp asymptotics of the stability constants and condition numbers of polynomial B-spline bases (see, e.g., [28]).

5.4 The multivariate case

By now, the asymptotic theory developed by Daniels [6] has been been extended to the case of several variables, and several equivalent approaches have been used for deriving multivariate saddlepoint approximations - the method of steepest descent for Laplace integrals of functions of several complex variables, the Morse lemma, special cases of multivariate generalized Edgeworth asymptotic expansions, Esscher tilting, etc. (see [21], [4], [15]). This mathematical apparatus suffices to extend the results from our section 4 to all kinds of multivariate B-splines and respective interpolations (see, e.g., [5] for a diversity of multivariate interpolations). In all these cases the multivariate B-spline is considered as a particular case of density of an absolutely continous cumulative distribution function uniquely determined by the knot distribution and the types of interpolatory functionals. In all cases the main term of the generalized Edgeworth asymptotic expansion is determined by an appropriately dilated, translated and factored multivariate Gaussian and the Legendre transform of the respective strictly convex multivariate cumulant generating function. In the particular case of saddlepoint approximation, the dependence on the Gaussian is eliminated. The results of a detailed study of the general multivariate asymptotic expansion, and the particular characterization of the cumulant generating function for the different types of multivariate interpolations in [5], will be presented elsewhere.

The definition of *tensor-product* ERBS is quite straightforward (see [19]). The diversity of possible finite or infinite dimensional local spaces allows for an easy extension of the finite dimensional tensor-product ERBS to infinite dimensional ERBS for Gordon hypersurfaces and Boolean sums of ERBS for any number of variables.

In Figure 4 is given a 3x3 tensor-product ERBS surface in Bezier form with its Bezier control polyhedron. The local curves in each of the 2 parameters of the surface are quadratic Bezier curves. The control polyhedron is determined by 81 3D-points (corresponding to the control polyhedra of 9 3x3 Bezier tensor-product patches 'ERBS-blended' together in one surface).

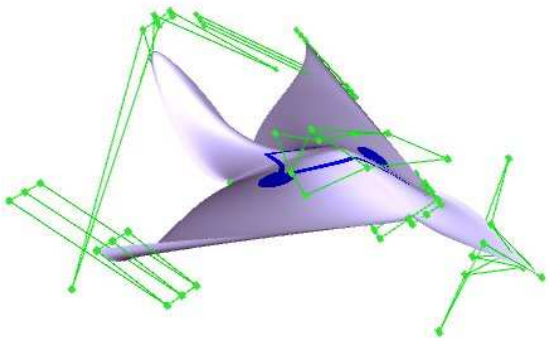

Figure 4: A tensor-product ERBS surface with its Bezier control polyhedron

Another m-variate ERBS is the *star-shape supported* ERBS obtained from a radial ERBS where the radius of support is made dependent on the $m-1$ angles in the m dimensional hyperspherical change of variables. It can be used in the context of Rvachev's R-functions (see, e.g., [26], [25] and subsection 3.2) for constructing finite or infinite dimensional spaces of interpolants for Dirichlet and Neumann boundary value problems on manifolds with a boundary.

A conspicuous example of the manifestation of the new 'super properties' of ERBS in the multivariate case is the construction of smooth B-splines on m-dimensional simplectifications (triangulations for $m=2$). The respective result for polynomial B-splines is given in [16]. This construction is masterful in many ways but, just as in the case $m=1$, for $m=2$ the B-spline of a C^l-smooth partition of unity over a triangulated polygonal domain in $\mathbb{R}^2$ must be supported on the whole $(l+1)$st neighbourhood of the vertex at which the B-spline is centred (see also [1]). This is not easy to implement already for $m=2$ and large l, and both the algorithmic and the computational complexity of the algorithm increases very rapidly with the increase of m and l. In the case of ERBS, it is possible to construct a C^∞-smooth partition of unity such that every B-spline is supported on the first neighbourhood of 'its' vertex, and has remarkable interpolatory properties. Here is an outline of this construction which we shall be able to describe explicitly for every dimension m.

Let $\Omega \subset \mathbb{R}^m,\ m=1,2,3,\ldots$, be a polygonal domain, and let $\Sigma(\Omega)$ be a non-degenerate m-dimensional simplectification of Ω (triangulation for $m=2$). Define a univariate ERBS in (1-2) by setting $n=1,\ t_k=k,\ k=0,1,2$. By (1), $B(t)=B_1(t)$ is the ERBS centered at $t=1$, supported at $[0,2]$, and having intrinsic parameters $\alpha=\alpha_0>0$, $\beta=\beta_0>0$, $\gamma=\gamma_0>0$, $\sigma=\sigma_0>0$, $\lambda=\lambda_0\in[0,1]$, for $t\in[0,1]$. (We shall not be interested in its intrinsic parameters for $t\in(1,2]$.) Let $T\in\Sigma(\Omega)$ be an m-dimensional simplex, and let $P_\mu,\ \mu=0,\ldots,m$, be the vertices of T in the affine frame $\{0,\mathbb{R}^m\}$. For $x_\mu\in\mathbb{R},\ \mu=0,\ldots,m$, such that

$$x_\mu\geq 0,\ \mu=0,\ldots,m,\ \text{and}\ \sum_{\mu=0}^{m} x_\mu = 1, \tag{55}$$

consider for $r=1,2,\ldots$ the identity

$$\left(\sum_{\mu=0}^{m} x_\mu\right)^{r-1} \frac{\sum\limits_{\mu=0}^{m} B(x_\mu)}{\sum\limits_{\mu=0}^{m} B(x_\mu)} \equiv 1, \tag{56}$$

and use the LHS (left-hand side) of (56) as a generating function, which yields the basis

$$b_{\rho,\nu}(x) = \frac{(r-1)!}{\prod\limits_{\sum_{\mu=0}^{m}\rho_\mu=r-1}\rho_\mu!}\left(\prod_{\sum_{\mu=0}^{m}\rho_\mu=r-1} x_\mu^{\rho_\mu}\right)\frac{B(x_\nu)}{\sum\limits_{\mu=0}^{m} B(x_\mu)}, \tag{57}$$

where ρ is a multiindex with $|\rho| = \sum_{\mu=0}^{m} \rho_\mu = r-1$, $\nu = 0, \ldots, m$, and the dimension of this basis is $(m+1)^r$. We shall call the elements of the linear span of this basis *Bezier ERBS macroelements over* T. In this setting, the classical *polynomial Bezier patches over* T (see [14]) correspond to the limiting value $\beta = 0$, in which case $B(t) \equiv 1$ on $[0,1]$ and the dimension of the basis in (57) reduces to $(m+1)^{r-1}$. Consider the (scalar or vector-valued) function defined over Ω by

$$f_\beta(y) = \sum_{\nu=0}^{m} \sum_{|\rho|=r-1} c_{\rho,\nu}(T) b_{\rho,\nu}(y),\ y \in T,\ T \in \Sigma(\Omega). \tag{58}$$

For the classical polynomial case $\beta = 0$, it is well known that if $r = 2, 3, \ldots$, then $f_\beta = f_0$ is analytic in the interior, and in general only C^0-continuous on the boundary, of any $T \in \Sigma(\Omega)$, hence, on Ω as a whole. Moreover, if in the classical case $\beta = 0$ we have simple multiplicity $r = 1$, then: if $c_{00}(T)$ takes different values for different $T \in \Sigma(\Omega)$, then f_0 is discontinuous somewhere in Ω; if $c_{00}(T) = const$ for all $T \in \Sigma(\Omega)$, then $f_0 \in C^\infty(\Omega)$ but the case is trivial, since $f_0 \equiv const$ on Ω. If, however, $\beta > 0$ (the ERBS case), it is possible to construct a non-trivial C^∞-smooth partition of unity over Ω, such that for every $P \in \prod(\Sigma)$, defined by

$$\prod(\Sigma) = \{P : P \text{ is a vertex of } T \in \Sigma(\Omega)\}, \tag{59}$$

there exist a unique ERBS $B = B_P$ from the partition, which is supported at

$$star_1(P) = \cup\{T \in \Sigma(\Omega) : P \text{ is a vertex of } T\}, \tag{60}$$

satisfies

$$B_P(t) = \begin{cases} 0, & t \in \Omega \setminus star_1(P), \\ 1, & t = P, \\ \in (0,1), & t \in star_1(P) \setminus \{P\}, \end{cases} \tag{61}$$

$$B_P \in C^\infty(\Omega),\ \text{for every } P \in \prod(\Sigma), \tag{62}$$

and

$$\sum_{P \in \prod(\Sigma)} B_P \equiv 1 \text{ on } \Omega. \tag{63}$$

It is simplest to construct this partition of unity for the case of simple multiplicity in (56): $r = 1$ for all $T \in \Sigma(\Omega)$. Under this assumption consider f_β in (58) with the following selection of the coefficients $c_{\rho,\nu}(T) = c_{0,\nu}(T)$ given by

$$c_{0\nu}(T) = \begin{cases} 0, & T \subset \Omega \setminus star_1(P), \\ 0, & T \subset star_1(P), \quad \nu \neq \nu_P(T), \\ 1, & T \subset star_1(P), \quad \nu = \nu_P(T), \end{cases} \tag{64}$$

where $\nu_P(T)$ is the unique value of $\nu = 0, \ldots, m$, for which the barycentric coordinates $x_\nu = 0,\ \nu = 0, \ldots, m$, $\nu \neq \nu_P(T)$, $x_\nu = 1$, $\nu = \nu_P(T)$, correspond to the vertex P of $T \subset star_1(P)$. It can be verified that the family $B_P,\ P \in \prod(\Sigma)$, satisfies (60-63), and it can also be seen that these properties are the extensions of P1-P3, P5 of section 2. The reader is invited to verify also that, for $f_\beta = B_P$, f_β is analytic in the interior of every $T \in \Sigma(\Omega)$ and C^∞-smooth on Ω. In Figure 5 and 6 are given the 3D-plot and height colour map, respectively, of a C^∞-smooth ERBS, minimally supported at the $star_1$-neightbourhood of 'its' vertex in the triangulation.

Note also that the new ERBS in Figure 5,6 provides an important particular instance of a *star-shape supported* ERBS, in the sense specified above.

A very remarkable and useful 'superproperty' of the new ERBS over triangulations is that all the normal derivatives of f_β, of every order, vanish everywhere on the boundary of every $T \in \Sigma(\Omega)$. Moreover, the trace of this ERBS on lower-dimensional simplectic parts of the boundary of a simplex also retains this remarkable property. For example, consider a tri-variate ERBS over a 3D simplectification via tetrahedra. Then: the normal derivatives of every order of the ERBS will vanish on the boundary of every polyhedron of the simplectification; the normal derivatives of every order of the bi-variate trace of the ERBS on every triangle side of the boundary of every such tetrahedron will also vanish; the derivatives of every order of the uni-variate trace of the ERBS on every edge of the tetrahedron will also vanish at the two boundary vertices. Note that this is the analogue of P4, section 2, for the present case. The fact that all B_P are supported at $star_1(P)$ for all polygonal $\Omega \subset \mathbb{R}^m$ and all respective simplectifications $\Sigma(\Omega)$ which are non-degenerate (i.e., the m-dimensional volume for every $T \in \Sigma(\Omega)$ is strictly positive), is another manifestation of a "superproperty" of ERBS, compared to polynomial B-splines for which this property is not available in general (see [1]).

Once we have constructed the partition $B_P,\ P \in \prod(\Sigma)$, satisfying P1-P5 for the present context, let us discuss the local functions/curves, i.e., the analogue of (3). Here we shall restrict the consideration only to polynomial curves, i.e., the analogues of (50) and (53).

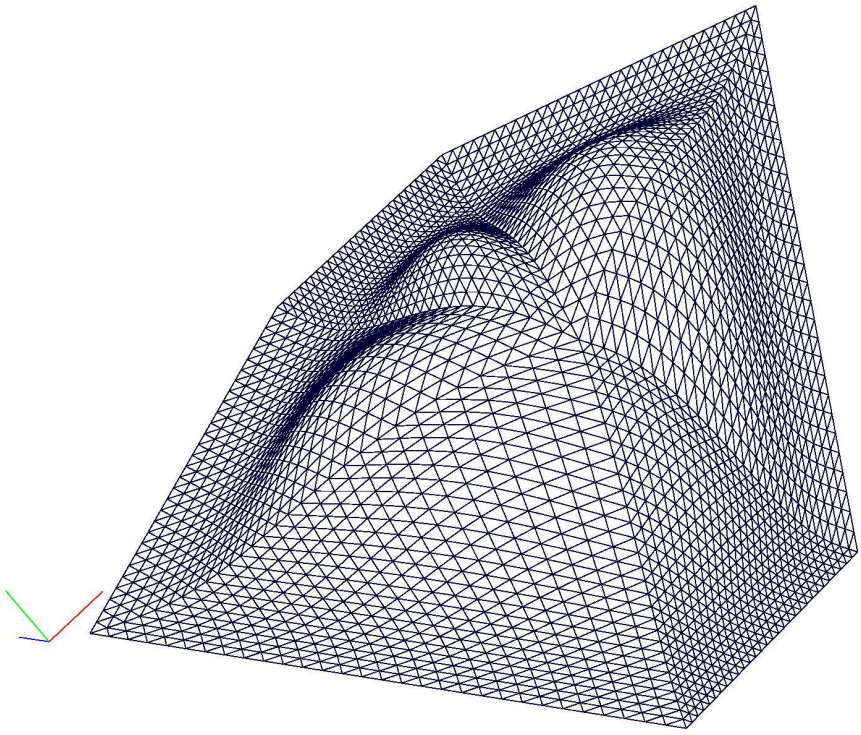

Figure 5: 3D-plot of a C^∞-smooth ERBS minimally supported over the $star_1$-neighbourhood of 'its vertex in a triangulation. The collection of these ERBS for every vertex in the triangulation provides a C^∞-smooth partition of unity over this triangulation.

Besides the local barycentric coordinates $x_i,\ i = 0, \ldots, m$, for every $T \in \Sigma(\Omega)$, we can introduce also global cartesian coordinates $y = (y_1, \ldots, y_m) \in \Omega$, since $\Omega \subset \mathbb{R}^m$. For every $P \in \prod(\Sigma)$ consider $r_P = 1, 2, \ldots$, and define the m-variate Taylor monomial basis centered at $P = (y_{P1}, \ldots, y_{Pm})$ with total degree not bigger then $r_P - 1$, as follows

$$H(P, \rho; y) = \frac{\prod_{j=1}^m (y_j - y_{Pj})^{\rho_j}}{\prod_{j=1}^m \rho_j!}, \quad y \in \mathbb{R}^m, \tag{65}$$

where $\rho = (\rho_1, \ldots, \rho_m)$ is a multiindex, with

$$\rho_j \geq 0,\ j = 1, \ldots, m,\ \sum_{j=1}^m \rho_j = |\rho| = 0, 1, \ldots, r_P - 1. \tag{66}$$

From here we get the following Hermite interpolatory form

$$f(y) = \sum_{P \in \prod(\Sigma)} \left[\sum_{|\rho|=0}^{r_P - 1} H(P, \rho; y) D^\rho g(y_{P1}, \ldots, y_{Pm}) \right] B_P(y), \tag{67}$$

where $y \in \Omega$ and $D^\rho g$ is the usual notation for the respective partial derivative of g. Formula (67) is analogue of (50) for this case. To obtain an analogue of (53) from here, we may proceed, as follows.

1. For $y \in T \in \Sigma(\Omega)$, make a change of coordinates, from the global cartesian coordinates $y_1, \ldots, y_m$ to the local barycentric coordinates $(x_0, \ldots, x_m)$. The total degree of the resulting polynomial space remains invariant, becase in this case the change of variables is affine.

2. In the local barycentric coordinates $(x_0, \ldots, x_m)$, for every vertex P of T, change the basis from the monomial basis in $x_0, \ldots, x_m$ of total degree not exceeding $r_P - 1$ to the Bernstein basis on T of degree $r_P - 1$, multiply by $B_{\nu_P}(x_{\nu_P})/[\sum_{\mu=0}^m B_\mu(x_\mu)]$, where ν_P was defined in (64), and sum over all vertices P of T; doing this for all $T \in \Sigma(\Omega)$, all coefficients $c_{\rho,\nu}(T)$ in (58) are computed in a unique way from the coefficients $D^\rho g(P),\ P \in \prod(\Sigma)$, of (67), and (58, 67) define the same $f \in C^\infty(\Omega)$. Note that there are also alternative possibilities to define a Bezier form (58) directly in the global variable $y \in \Omega$.

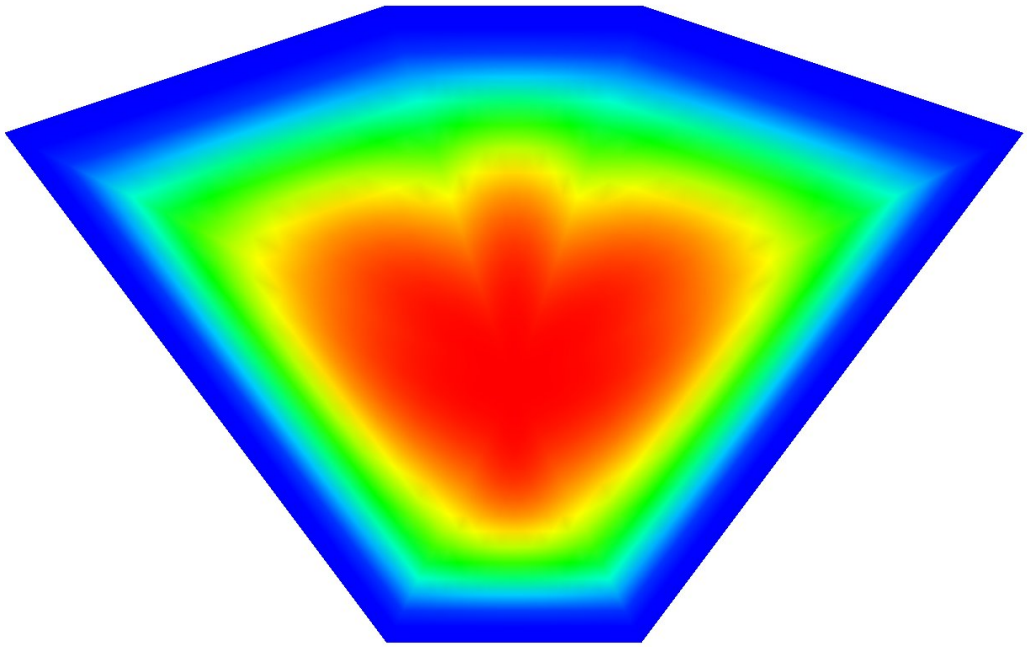

Figure 6: Spectral ('rainbow') colour height map of the ERBS in Figure 5. The map is in the plane $0xy$, 'blue' corresponds to the minimal height level $z = 0$, 'green' corresponds to the median $z = \frac{1}{2}$, and 'red' corresponds to the maximal level $z = 1$. This type of colour maps are referred to as 'colour (mode 1) maps' in [10].

Let us note that, once the axes of the global cartesian coordinates are selected, it is possible to extend the simplectified polynomial domain to a (minimal) hyper-rectangle with axes parallel to the selected ones for the global coordinates. If we add the vertices of the hyper-rectangle to the vertices of the simplectification, we can generate an extended simplectification over the hyper-rectangle which agrees with the original one on the original polygonal domain (assuming that the simplectification process is unique, which would be the case, e.g., with the Delaunay algorithm). Then using the Hermite interpolatory property of ERBS of both tensor-product type and on the simplectification, it is easy to 'convert' the triangulated ERBS hypersurface into a tensor-product one, and vice versa. An example is given in Figure 9. In the LHS is given a (scalar-valued) triangulated ERBS surface; in the RHS the polygonal domain is extended to a (minimal) rectangle. (This means that more ERBS basis functions will be added to the basis providing C^∞-smooth partition of unity over the extended triangulation.) The resulting triangulated surface can easily be approximated by tensor-product ERBS in Herimite interpolatory form. (Of course, the quality of this interpolation depends on the selection and dimension of the univariate ERBS bases in every variable and the depth of the Hermite interpolation. It can also be improved considerably, e.g., by using Hermite interpolatory Gordon surfaces.)

Finally, let us note also that the requirement about certain order of smoothness of the polynomial B-splines leads to fairly complicated interpolatory structures (see [17],[2],[18]) while ERBS exhibit again a "superproperty" in the sense that property P4 in this context also leads us to the following observation. In (58), consider $c_{\rho,\nu}$ to be regularized quasi-interpolatory functionals of the type proposed in [16]. *Every such regularized quasi-interpolation for f_b in (58), $\beta > 0$, on an m-dimensional simplex T_m or part of the $(m-1)$-dimensional hypersurface boundary $\partial(T)$ of $T_m \in \Sigma(\Omega)$ can be reduced to a respective interpolation on the $m+1$ vertices of T_m. In particular, all boundary-value problems of Dirichlet and Neumann type of every order on the polygonal boundary $\partial(\Omega)$ of Ω for f_β, $\beta > 0$, can be reduced to interpolation problems only on the vertices P of $\partial(\Omega) : P \in \prod(\Sigma) \cap \partial(\Omega)$.* These new problems may involve antiderivatives of f_β on the vertices.

This observation can be proved by iterative application of the Stokes theorem, starting from the m-dimensional volume T_m and ending with an application of the Newton-Leibniz theorem on the 1D edges of T_m. At every such iteration the normal derivatives vanish everywhere on the boundary, which simplifies considerably the computations.

All these remarkable facts are a manifestation of new 'super properties' of ERBS, unavailable for polynomial B-splines.

More details about this and two other constructions of smooth ERBS partitions of unity on triangulations

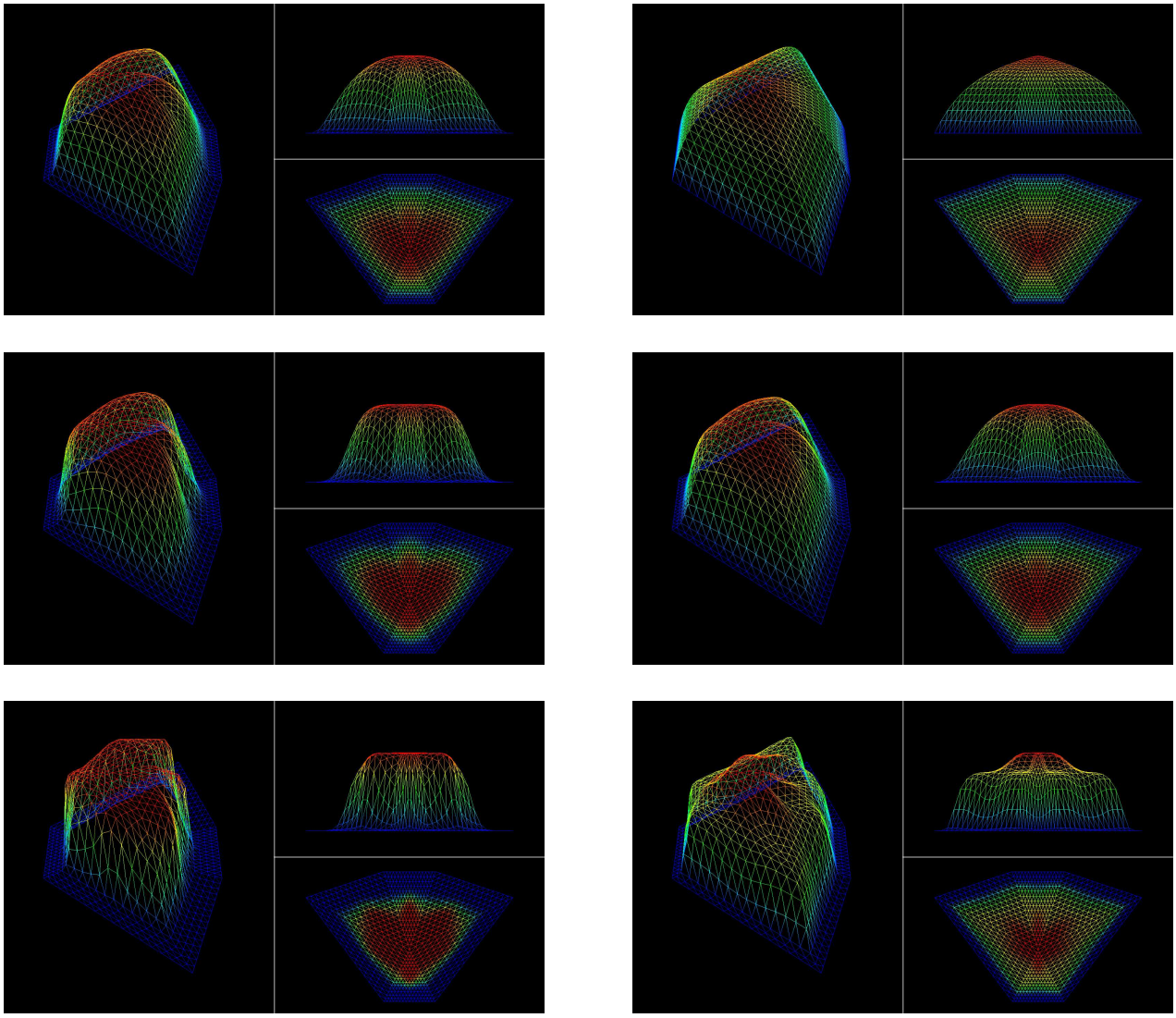

Figure 7: The ERBS of Figure 5 and Figure 6 for different sets of intrinsic parameters: cases a-f in Table 1 and Figure 1

will be given elsewhere.

5.5 Differential geometry

Thanks to the Hermite interpolation property up to every available order, ERBS curves, surfaces and higher-dimensional manifolds have a very simple intrinsic structure.

1. ERBS interpolate every available instrinsic differential structure at the knots, e.g.: for curves, the Frenet frame, the curvature, the torsion, etc.; for surfaces, the tangential plane, the normal vector, the coefficents of the first and second fundamental form, the principal, Gaussian and mean curvatures, and so on. The values of all of these quantities do not depend on the intrinsic parameters of the ERBS involved.

2. Outside of the knots, ERBS interpolate the intrinsic geometry at the knots in a C^∞-smooth way which depends on the intrinsic parameters of the ERBS involved.

For more details, see [11], section 5.

5.6 Rational form

The rational form of ERBS, which we call NUERBS, by analogy with NURBS, will be discussed in detail elsewhere. First results are obtained in [11]. Here we make only the following remarks.

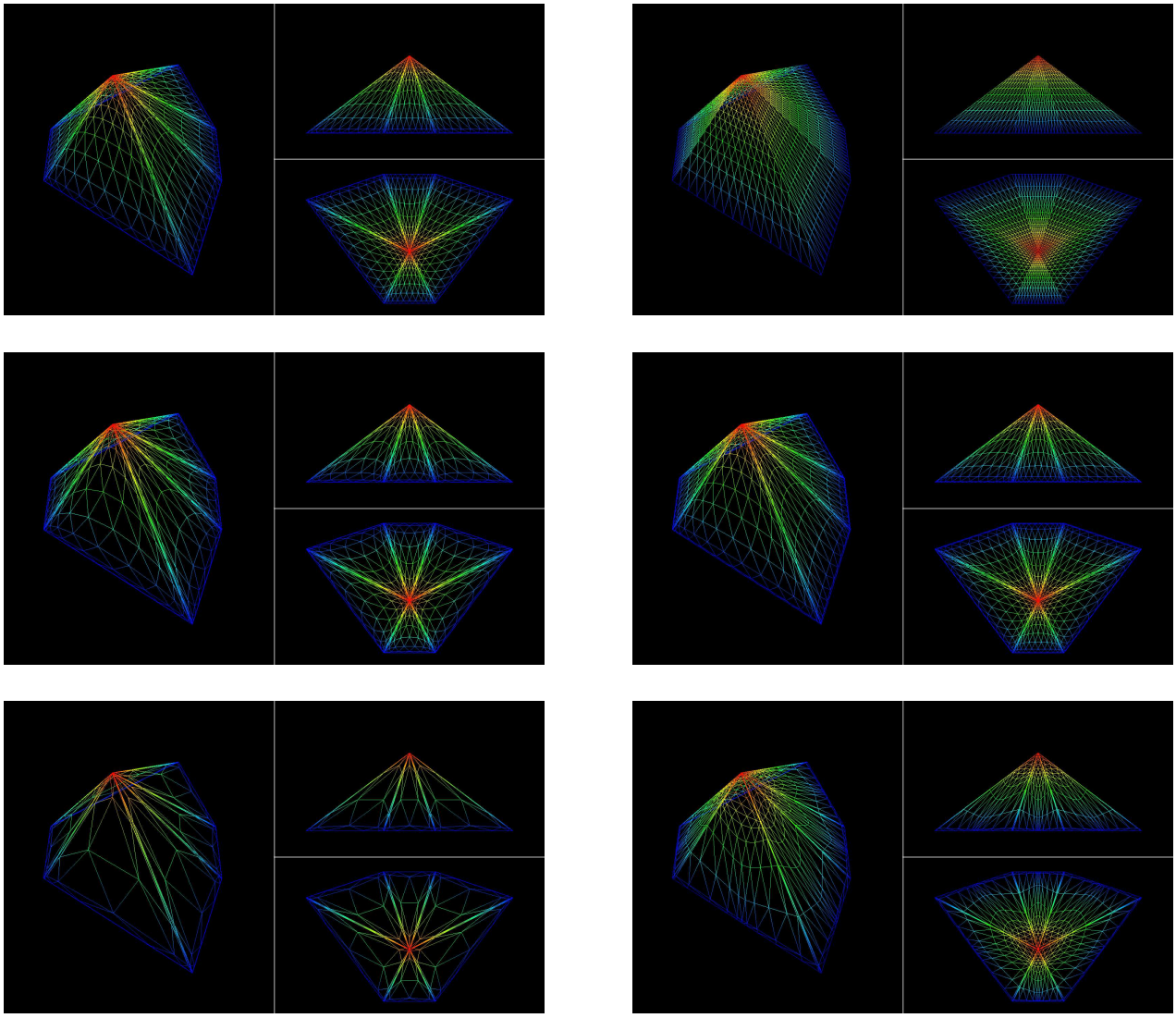

Figure 8: The ERBS of Figure 7 (cases a-f in Table 1 and Figure 1) plotted as scalar-valued Lagrange interpolants: the graph is that of the respective piecewise linear B-spline over the $star_1$-neighbourhood of the considered vertex in the triangulation; note the variation of the C^∞-smooth parametrization in the six cases.

The general NUERBS form is defined for the maximal subspaces $\mathcal{F}(B_k)$, $k = 1, \dots, n$, in subsection 5.1, as follows.

$$f(t) = \frac{\sum\limits_{k=1}^{n} l_k(t) W_k B_k(t)}{\sum\limits_{j=0}^{n} W_j B_j(t)}, \qquad t \in [t_1, t_n], \tag{68}$$

where $W_j > 0,\ j = 1, \dots, n$. For specific finite-dimensional subspaces of $\mathcal{F}(B_k)$ it is possible to define a hierarchy of NUERBS forms, of which the general form (68) is always the simplest. As with NURBS, the weights W_j are used for fine control over the curve/surface. This control, in the case of NUERBS, is shared with the intrinsic parameters of the ERBS $B_k,\ k = 1, \dots, n$. The role of the weights W_j is in some sense dual to that of the intrinsic parameters. This can be clearly seen if we try to introduce a rational form in (57). Then it becomes clear that this is only possible if every vertex $P \in \prod(\Sigma)$ is assigned its own weight W_P, and every simplex $T \in \Sigma(\Omega)$ - its own set of intrinsic parameters. In the case of Lagrange interpolation with ERBS, variations of the weights of the rational form and the intrinsic parameters do not change the form of the graph (which is the one of the piecewise linear Lagrange B-spline interpolant), but they do exercise mutually dual control over the parametrization on the graph. In the case of curves, this is illustrated on Figure 10. In the top level is given the NUERBS for the Lagrange interpolant at three points for these different sets of weights (left: $(1, 0.5, 1)$, middle: $(1, 1, 1)$, right: $(1, 5, 1)$). The intrinsic parameters of all three ERBS are default (case a in Figure 1). The result is: increasing the weight in a knot slows down the parametrization (denser means slower). In the bottom level

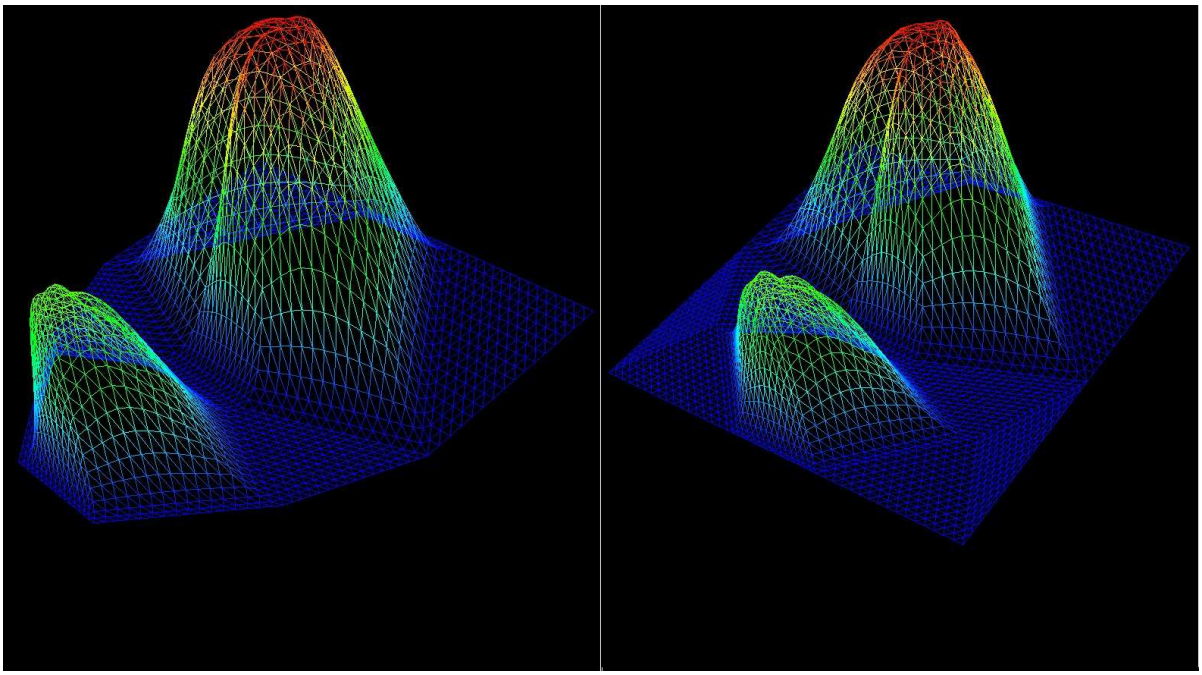

Figure 9: Approximate conversion between triangulated and tensor-product ERBS surfaces via Hermite interpolation. Left: triangulated polygonal domain. Right: extension of the triangulation to a minimal rectangle containing the original domain. The approximated tensor-product or Gordon surface can now be obtained by Hermite interpolation.

is given the Lagrange interpolant (NUERBS with vector of weights $(1,1,1)$) for three different selections of the intrinsic parameters of the ERBS at the last interpolation knot, i.e., in the right-hand segment (left: case b of Figure 1; middle: default (case a of Figure 1); right: case f of Figure 1); the intrinsic parameters at the other two knots are default (case a of Figure 1). (Thus, the middle cases at the top and bottom rows are the same.) The result at the bottom row: change of the speed of parametrization within the right segment; the left segment remains unchanged.

Figures 11-13 provide an analogue of Figure 10 for NUERBS over triangulations. Here we consider a rational form such that every vertex in the triangulation has its own assigned weight which appears in the rational form of (56) and (57) in every triangular patch adjacent to the vertex. In Figure 11 is given the parametrization of the Lagrange interpolant when all ERBS have default intrinsic parameters (case a in Figure 1) and all vertices in the triangulation have weights equal to 1. In Figure 12 the intrinsic parameters are the same as in Figure 11, but two of the weights are increased. In Figure 13, the weights are the same, but the intrinsic parameters for two of the triangles are modified. For one of these two triangles, they are modified to case b in Figure 1; for the other one of these two triangles - to case f in Figure 1.

The NUERBS form of multilevel ERBS can be considered as (a truncation of) an infinite chain fraction.

5.7 Cardinal ERBS

Some new properties of cardinal ERBS are, as follows.

For $f \in S(\mathbb{R})$ (the Laurent Schwartz space), (51) can be extended to

$$\begin{aligned} f(t) = \sum_{k=-\infty}^{\infty} \left[\sum_{j=0}^{\infty} \frac{(t-k)^j}{j!} f^{(j)}(k) \right] B(t-k) = \\ = \sum_{j=0}^{\infty} \tfrac{1}{j!} \left[g_j * f^{(j)} \right](t) = \left\{ \left[\sum_{j=0}^{\infty} \tfrac{(-1)^j}{j!} g_j^{(j)} \right] * f \right\}(t), \quad t \in \mathbb{R}, \end{aligned} \tag{69}$$

where

$$\varphi * \varphi(t) = \int_{-\infty}^{\infty} \varphi(\theta)\psi(t-\theta)d\theta, \quad g_j(\theta) = \theta^j B(\theta), \tag{70}$$

and

$$\sum_{j=0}^{\infty} (-1)^j g_j^{(j)}/j! = \delta \text{ in } S'(\mathbb{R}) \tag{71}$$

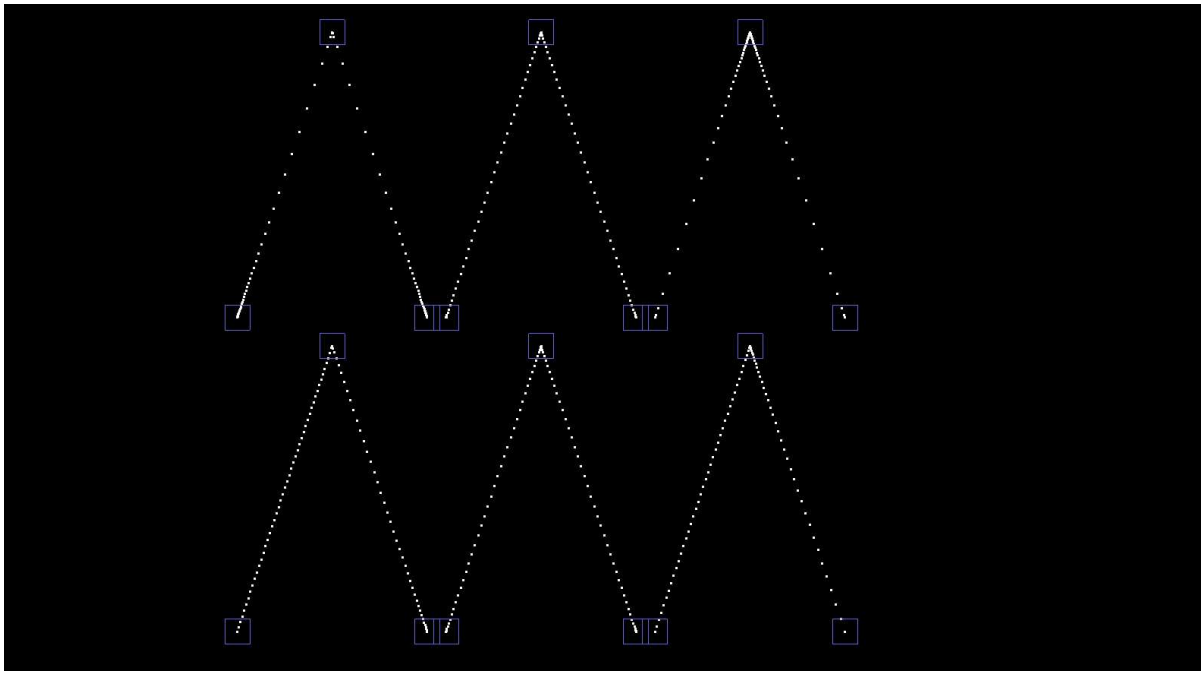

Figure 10: Dual control via weights of rational form and intrinsic parameters. Top level: control in the vertices via weight variation. Bottom level: control in the edges via intrinsic parameters of the ERBS.

(the space of moderate distributions, dual to $S(\mathbb{R})$), where δ is Dirac's delta function on $\mathbb{R}$.

The sampling formula (69) can be used to define a special type of multilevel splines - orthogonal and biorthogonal ERBS multiwavelets which display similar 'super properties' compared to spline wavelets as ERBS compared to polynomial B-splines and NUERBS compared to NURBS. For example, for ERBS multiwavelets it is possible to define a rational (NUERBS) form. ERBS multiwavelets will be studied in detail elsewhere.

6 Computational aspects

6.1 Differentiation and integration

Let us consider the notation in (41). One straightforward way is to compute the derivatives of $B^{(j)}(t)$ recursively. A more technical and lengthy computation shows that the $m+1$-st derivative of the ERBS (the m-th derivative of the exponential expression in (41) can be computed in a reasonably compact closed form. In fact, the idea of this computation can be extended to provide a closed form also for the $m+1$-st derivative of the general non-parametric ERBS. We shall present these formulae and their derivations elsewhere.

$B(t)$ is analytic and is expandable in a series which, together with its derivatives of every order, converges uniformly on every compact in (a,b); the Taylor series for the exponent is outperformed by Padé approximations. In the computation of $B(t)$ and its antiderivatives we always use numerical integration. Since the integrand is C^∞-smooth, we use Romberg integration in all cases. The number of Romberg iterations is variable, depending on how close to the knots a or b B needs to be computed, and on the values of the intrinsic parameters α, γ and, to a lesser extent, β.

6.2 Computing ERBS near the knots

When t is near enough (depending on α, γ and β) to one of the knots (e.g., b), computation of $\varphi(t)$ will result in an underflow. In our programs (written in template-based C++) we deal with this on metaprogramming level, by exception handling within the definition of the respective template class. There are several ways to handle this.

1. The simplest one: whenever underflow occurs at this place, set the result to 0.

2. Depending on the smallest machine number $\varepsilon > 0$, write for $x > 0$ $e^{-x} = \left(e^{-\frac{x}{m}}\right)^m$, where $m = 2, 3, \ldots$, is such that $e^{-\frac{x}{m-1}} < \varepsilon \leq e^{-\frac{x}{m}}$. Compute $\prod_{k=1}^{m} e^{-\frac{x}{m}}$ by multiplication.

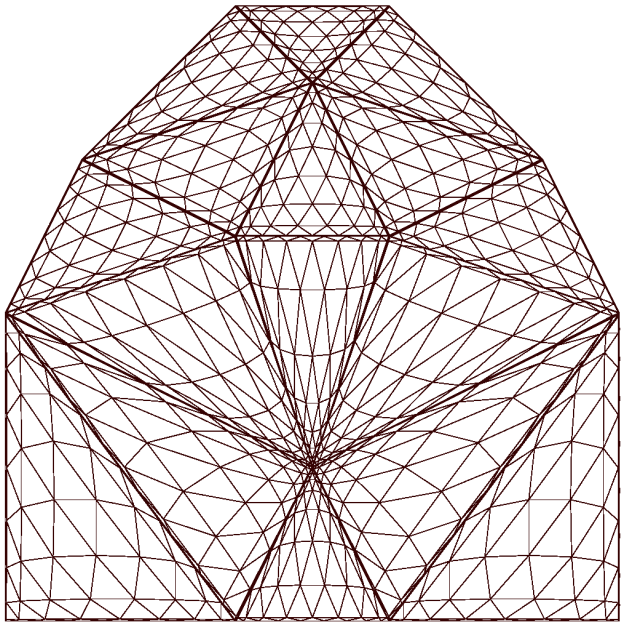

Figure 11: Dual control via NUERBS weights and ERBS intrinsic parameters: default weights; default intrinsic parameters

3. For t near b, approximate $\varphi(t)$ with a Birkhoff polynomial interpolant, as follows: Hermite interpolation at b, and Abel-Goncharoff interpolation away from b, the higher derivatives being interpolated further away from b.

4. Use a variable-bandwith Gaussian kernel smoother near b. This is the best method from the point of view of shape preserving, since it is based on the idea of Corollary 2.

Our experience is that, at the level of the current generation of computers, the simplest approach No. 1 is already quite sufficient. In our present software application for modelling curves and surfaces (see [19]) we use '1' and a modified version of '2' which will be discussed in detail elsewhere.

6.3 Computing roots and intersections

In the case of polynomials or locally polynomial functions (such as B-splines) of one real variable, when localizing the roots (real or complex) of an equation in an intersection problem, the emphasis is usually on numerical methods exploiting the polynomial algebraic structure of the equation. However, when studying multivariate intersection problems, with the increase of the dimension the emphasis is being shifted towards piecewise linearization or polylinearization (marching cube algorithms, etc.). Piecewise linearization is generally not a preferred technique for polynomial curves, because the quality of its results depends essentially on the quality of interpolation or fitting of the polynomial curve with a piecewise linear curve, which may vary a lot. This situation changes when the polynomial curve is taken in Bezier form, due to the variation diminution property. Thanks to it, the control polygon of a Bezier curve is known to be always a good initial point of a rapidly converging iterative process of approximating the curve with a piecewise linear curve (say, by appropriate corner cutting). This process can be used for localization of intersections (roots of equations).

B-spline curves also enjoy the variation diminution property, and the piecewise linearization technique is readily available for them. For the low-degree polynomical B-splines that are mostly used in applications, however, the algebraic methods are preferable, in view of the low degree of the polynomial equations to be solved locally in these cases. However, when the degree of the B-spline begins to increase, so does the degree of the local equations, and, especially in dimensions 3 and higher, the piecewise linearization technique soon tends to become superior in efficiency, compared to algebraic methods. Since ERBS preserve the variation diminution property of polynomial B-splines, and in view of the fact that ERBS are the asymptotic limits of polynomial B-splines as the degree of the latter tends to infinity, the above arguments imply that piecewise linearization is a good universal choice for localization of roots and intersections in the case of ERBS, for curves, surfaces or volume deformations alike. In the case of ERBS, iterative processes for approximating the ERBS curve/surface starting

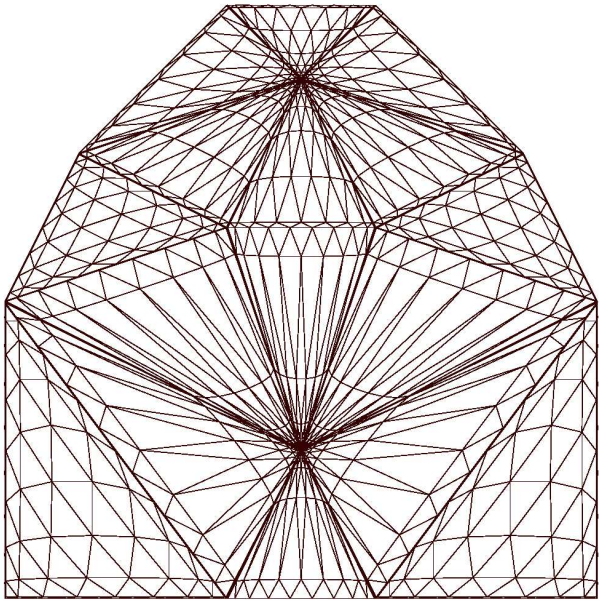

Figure 12: Dual control via NUERBS weights and ERBS intrinsic parameters: modified weights; default intrinsic parameters

from its Bezier control polygon/polyhedron are more rapidly converging than their analogues with polynomial B-splines, which follows from the specific of the variation diminution property of the faster bending ERBS, as discussed in subsection 5.3. Once the intersection points are localized by solving the local linear or polylinear equations arising in the problem for intersection of piecewise linear manifolds, any hill-climbing iterative method (e. g., Newton's method and its various enhancements) can be used for high-precision computation of the intersections. Moreover, since ERBS are C^∞-smooth, Aitken-Steffensen convergence acceleration procedures are very efficient with ERBS (cf. the discussion about Romberg integration in subsection 6.1).

6.4 Algorithmic versus computational complexity

A decade ago, ERBS would have still been expensive to compute in industrial applications. Nowadays, with the super-fast hardware-supported computation of the exponent and many other new features, the computation of ERBS is already approaching the speed of computation of classical B-splines. At the same time, it was shown in the previous section 5 that the ERBS algorithms tend to be simpler, more straightforward and easier to program than the algorithms of classical B-spline theory, and these advantages of ERBS tend to increase with the increase of the number of variables. This, together with the best possible localization of support of ERBS, offers nowadays a good tradeoff. Note also the ready parallelization, hence, easy and efficient scalability, of the ERBS algorithms. What is more, ERBS are 'on the correct side of technological progress' - the more our computers become advanced, the more will the aspects be in which ERBS outperform polynomial B-splines. In our opinion, the rational form of ERBS, NUERBS, has the potential to replace NURBS as industrial standard in CAGD whitin the next 5-10 years.

A detailed comparative study of the computational complexity of ERBS versus polynomial B-splines will be performed elsewhere. We intend to compare the results with respect to the Traub-Wozniakowski and Renegar and Neff approaches to measuring complexity, with different weights of operations, corresponding to the evolution of the state of the art of scientific computing from 1990 until today.

7 Applications

The range of potential applications of ERBS is vast. Here are several examples, starting with the topics in Section 3 which motivated the research on ERBS in the first place.

1. ERBS can be used as C^∞-smooth partition of unity in the concept of *diffeomorphic splines* (see [7], subsection 4.2) which can be used for parametrization of differentiable manifolds. This can be

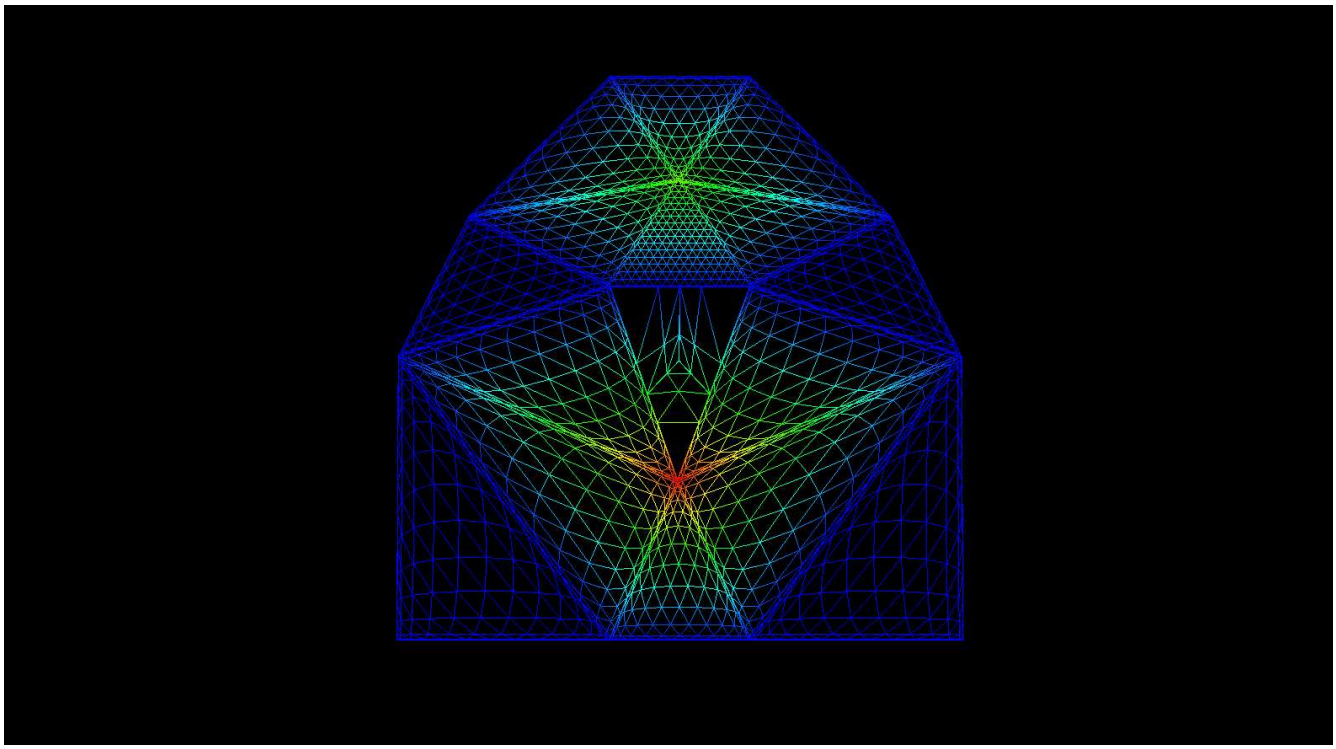

Figure 13: Dual control via NUERBS weights and ERBS intrinsic parameters: default weights; modified intrinsic parameters

used for data interpolation and optimal data fitting by smooth manifolds, with applications, e.g., to medical imaging (see also subsection 3.2, [25] and [26]).

2. ERBS have also very interesting theory as functions of a complex variable. In particular, they can be used for efficient computation of functions of matrices, using the formula for the F. Riesz - Dunford integral representation mentioned in subsection 3.3. In the case of 2,3 and 4 dimensions (which includes all dimensions of interest for CAGD) the eigenvalues of the matrices can be computed in radicals from the matrix coefficients, which allows an explicit representation of any analytic function of these matrices in closed form. (See also subsection 3.3.) These results can be used also to improve the currently available results on computation of the uniform operator norm of operator resolvents and other analytic functions of operators. (See also subsection 3.4) In particular, the explicit computation of the exponent of an $n \times n$ matrix, $n = 2, 3, 4$, together with the results in [7], makes it possible to achieve explicit and computationally efficient closed-form parametrization of all global diffeomorphisms on the closed unit ball in $\mathbb{R}^n$, at least for $n = 1, 2, 3, 4$. (See also subsection 3.2).

3. ERBS can be used for modelling of surfaces with edges, wedges, ridges, canyons, shockwave fronts, etc., as well as for performing cuts, changing topological genus or orientability of manifolds, etc. The current industrial standard for geometric modelling of such surfaces are NURBS, which require the generation of several smooth NURBS surfaces which are then "glued" together along the respective curve of singular points. In the case of ERBS, a single ERBS C^∞-smooth surface is generated. Using only its control points, it can be modelled to fit (with any needed precision) the respective singularity fronts, while still remaining C^∞-smooth everywhere.

4. ERBS can be used as universal Riesz basis in the Besov and Triebel-Lizorkin space scales for the total range of the regularity index and the metric indices of these scales. In comparison, polynomial splines and wavelets provide such Riesz bases only for a limited range of these indices. As a consequence, ERBS can be used as universial finite and boundary element spaces in solving linear and nonlinear operator equations with possibly unbounded, densely defined operators, in particular, ODE and PDE of arbitrary order. In connection with parallel computing, currently a lot of research effort is being concentrated on the problem of scalable linear solvers (see, e.g., http://www.llnl.gov/groups/casc-sag.html). Because of the extreme localization of their support and their applicability to solving differential equations of any order, ERBS have the potential to 'trivialize' the problem about scalable linear solvers, since for the ERBS bases the matrices of the equation systems are always band-limited,

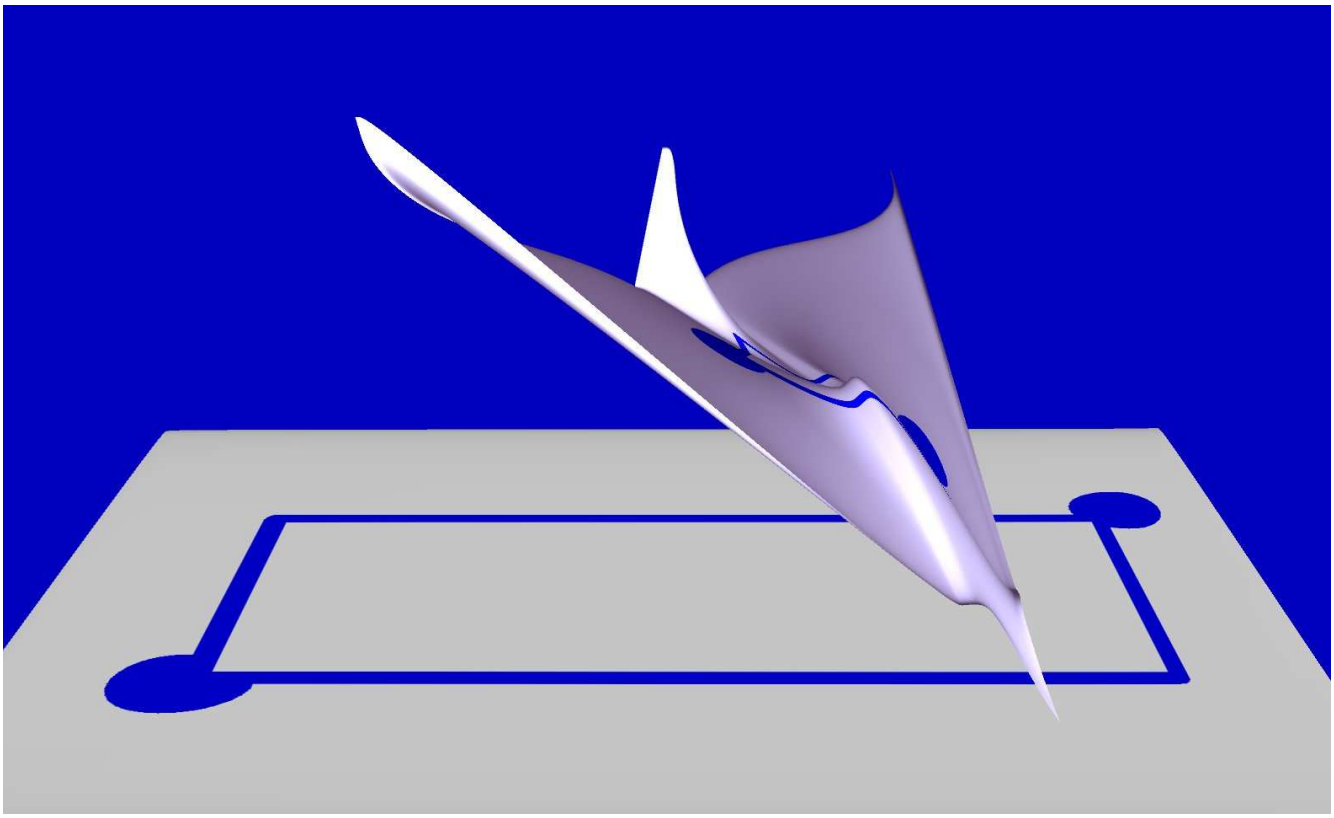

Figure 14: The initial and finite stage of the interactive modelling of an ERBS tensor-product surface in Bezier form (see Figure 4)

and scalability theory of linear solvers for systems of linear equations with band-limited sparse matrices is well developed by now. Moreover, if the simple multiplicity (Lagrange interpolation) ERBS basis is used, then the bandwidth of the band-limited matrices for ERBS FEM/BEM does not depend on the order of the ODE/PDE but only on the number of variables. (For example, with ODE of arbitrary order, the ERBS basis with multiplicity 1 will always generate a tridiagonal stiffness matrix.) This makes the problem about preconditioning ERBS FEM/BEM very interesting and important (see also the end of subsection 5.3).

8 Conclusion

On special occasions, special people deserve special presents.
Happy 60-th Anniversary, Tom!
The expo-rational B-spline is our present to you.

References

[1] Alfeld, P., and L. L. Schumaker, Non-existence of star-supported spline bases, SIAM J. Math. Anal. **31** (2000) 1482-1501.

[2] Alfeld, P., and L. L. Schumaker, Smooth macro-elements based on Powell-Sabin triangle splits, Adv. in Comp. Math., **16** (2002) 29-46.

[3] Bandtlow, O. F., Estimates for norms of resolvents and an application to the perturbation of spectra, Math. Nachr., **267(1)** (2004) 3-11.

[4] Bleistein, N., and R. A. Handelsman. Asymptotic Expansions of Integrals, Dover, New York, 1986.

[5] Bojanov, B. D., H. A. Hakopian, and A. A. Sahakian, Spline Functions and Multivariate Interpolations, Kluwer, Dordrecht, 1993.

[6] Daniels, H. E., Saddlepoint approximations in statistics, Annals Math. Statist., **25** (1954) 631-650.

[7] Dechevsky, L. T., Integral representation of local and global diffeomorphisms, Nonlinear Anal. Real World Appl., **4(2)** (2003) 203-221.

[8] Dechevsky, L. T., and L.-E. Persson, Sharp generalized Carleman inequalities with minimal information about the spectrum, Math. Nachr., **168** (1994) 61-77.

[9] Dechevsky, L. T., and L.-E. Persson, On sharpness, applications and generalizations of some Carleman type inequalities, Tôhoku Math. J., **48** (1996) 1-22.

[10] Dechevsky, L. T., and J. Gundersen, Isometric conversion between dimension and resolution, in Mathematical Methods for Curves and Surfaces: Tromsø 2004, M. Dæhlen, K. Mørken, L.L. Schumaker (eds.), Nashboro Press, Brentwood TN, 2005, pp. 103-114.

[11] Dechevsky, L. T., A. Lakså, and B. Bang, NUERBS form of expo-rational B-splines, Preprint No. 1/2004, Applied Mathematics, Narvik University College, ISSN 1504-4653.

[12] Dunford, N., and J. T. Schwartz, Linear Operators, Part I: General Theory, Wiley, New York, 1988.

[13] Dunford, N., and J. T. Schwartz, Linear Operators, Part II: Spectral Theory: Self Adjoint Operators in Hilbert Space, Wiley, New York, 1988.

[14] Farin G., Curves and Surfaces for CAGD. A Practical Guide, Morgan Kaufmann & Academic Press, San Francisco, 2002.

[15] Jensen, J. L., Saddlepoint Approximations, Clarendon Press, Oxford, 1995.

[16] Lai, M.-J., and L. L. Schumaker, On the approximation power of bivariate splines, Adv. in Comp. Math., **9** (1998) 251-279.

[17] Lai, M.-J., and L. L. Schumaker, Macro-elements and stable local bases for splines on Clough-Tocher triangulations, Numer. Math., **88** (2001) 105-119.

[18] Lai, M.-J., and L. L. Schumaker, Macro-elements and stable local bases for splines on Powell-Sabin triangulations, Math. Comp. **72** (2003) 335-354.

[19] Lakså, A., B. Bang, and L. T. Dechevsky, Exploring expo-rational B-splines for curves and surfaces, in Mathematical Methods for Curves and Surfaces: Tromsø 2004, M. Dœhlen, K. Mørken, L.L. Schmaker (eds.), Nashboro Press, Brentwood TN, 2005, pp253-262.

[20] Lyche, T., and K. Mørken, Theory and Application of Splines. Compendium, University of Oslo.

[21] McCullagh, P., Tensor Methods in Statistics, Chapman and Hall, London, 1987.

[22] Newman, D., Rational approximation to $|x|$, Michigan Math. J., **11** (1964) 11-14.

[23] Nikol'skii, S. M., Approximation of Functions of Several Variables and Imbedding Theorems, Springer, New York, 1975.

[24] Richards, F. B., and I. J. Schoenberg, Notes on spline functions. IV. A cardinal spline analogue of the theorem of the brothers Markov, Israel J. Math., **16** (1973) 94-102.

[25] Rvachev, V. L., T. I. Sheiko, and V. Shapiro, Generalized interpolation formulae of Lagrange-Hermite on arbitrary loci, J. Mechanical Engineering, National Academy of Science of Ukraine, **1(3-4)** (1998) 150-166.

[26] Rvachev, V. L., T. I. Sheiko, and V. Shapiro, Application of the method of R-functions to the integration of partial differential equations, Cybernet. Systems Anal. **35(1)** (1999) 1-18.

[27] Saff, E. B., R. S. Varga, and W. C. Ni, Geometric convergence of rational approximations to e^{-z} in infinite sectors, Numer. Math., **26** (1976) 211-225.

[28] Scherer, K., and A. Yu. Shadrin, New upper bound for the B-spline basis condition number. II. A proof of de Boor's 2^k-conjecture, J. Approx. Theory, **99(2)** (2001) 217-229.

[29] Schoenberg, I. J., Notes on spline functions. I. The limits of the interpolating periodic spline functions as their degree tends to infinity, Indag. Math., **34** (1972) 412-422.

[30] Schoenberg, I. J., Cardinal interpolation and spline functions. II. Interpolation of data of power growth, Collection of Articles Dedicated to J. L. Walsh on his 75th Birthday, VIII, J. Approximation Theory **6** (1972) 404-420.

[31] Schoenberg, I. J., Cardinal interpolation and spline functions. IV. The exponential Euler splines, in Linear Operators and Approximation, P. L. Butzer, J. -P. Cahane, B. Szökefalvi-Nagy (eds.), Birkhäuser, Basel, 1972, pp. 382-404.

[32] Schoenberg, I. J., Notes on spline functions. III. On the convergence of the interpolating cardinal splines as their degee tends to infinity, Israel J. Math. **16** (1973) 87-93.

[33] Seal, H. L., Spot the prior reference, J. Inst. of Actuaries, Students' Soc., **10** (1951) 255-258.

[34] Spivak, M., A Comprehensive Introduction to Differential Geometry, Vol. 1, Publish or Perish, Houston TX, 1999.

[35] Stahl, H., Best uniform rational approximants of $|x|$ on $[-1, 1]$, Mat. Sbornik **183** (1992) 85-118.

[36] Stahl, H., Best uniform rational approximants of x^a on $[0, 1]$, Bulletin Amer. Math. Soc. **28** (1993) 116-122.

[37] Unser M., A. Aldroubi, and M. Eden, On the asymptotic convergence of B-spline wavelets to Gabor functions, IEEE Transact. Information Theory, **38(2)**(1992) 864-872.

[38] Vjacheslavov, N., On the uniform approximation of $|x|$ by rational functions, Dokl. Akad. Nauk SSSR, **220** (1975) 512-515.

Affiliations/Addresses

⋆ Lubomir T. Dechevsky
• R&D Group for Mathematical Modelling, Numerical Simulation & Computer Visualization • Institute for Information, Energy & Space Technology • Narvik University College ⋄ 2 Lodve Lange's St. ⋄ P.O.B. 385 ⋄ N-8505 Narvik, NORWAY ⋄ E-mail: `ltd@hin.no` ⋄ http://ansatte.hin.no/ltd/

⋆ Arne Lakså
• R&D Group for Mathematical Modelling, Numerical Simulation & Computer Visualization • Institute for Information, Energy & Space Technology • Narvik University College ⋄ 2 Lodve Lange's St. ⋄ P.O.B. 385 ⋄ N-8505 Narvik, NORWAY ⋄ E-mail: `ala@hin.no` ⋄ http://ansatte.hin.no/ala/

⋆ Børre Bang
• R&D Group for Mathematical Modelling, Numerical Simulation & Computer Visualization • Institute for Information, Energy & Space Technology • Narvik University College ⋄ 2 Lodve Lange's St. ⋄ P.O.B. 385 ⋄ N-8505 Narvik, NORWAY ⋄ E-mail: `bb@hin.no` ⋄ http://ansatte.hin.no/bb/